Investigation and Quantification of Boundary Reaction Effect on Solute Transport in a Circular Pipe Reactor - Application to Laminar and Turbulent Flows

by

STEVEN T. SETZER

B.S., Clarkson University, 1997

A thesis submitted to the

University of Colorado in partial fulfillment

of the requirement for the degree of

Master of Science

Department of Civil, Architectural, and Environmental Engineering

1999

This thesis entitled:

Investigation and Quantification of Boundary Reaction Effect on Solute Transport in a Circular Pipe Reactor - Application to Laminar and Turbulent Flows

written by Steven T. Setzer

has been approved for the Department of Civil and Environmental Engineering

_____

Chair of Committee

_____

Committee Member

Date _____

The final copy of this thesis has been examined by the signators, and we find that both the content and the form meet acceptable presentation standards of scholarly work in the above mentioned discipline.

Setzer, Steven (M.S., Civil Engineering)

Investigation and Quantification of Boundary Reaction Effect on Solute Transport in a Circular Pipe Reactor - Application to Laminar and Turbulent Flows

Thesis directed by Professor Harihar Rajaram

This thesis examines the effects of a boundary reaction on the effective one-dimensional transport parameters for a biofilm coated pipe reactor. Both laminar and turbulent flow conditions are explored. A particle tracking model is used to compute the effective transport parameters and is verified with analytical results for the laminar flow case.

After a sufficient development time elapses, the influence of the initial solute distribution becomes insignificant and the effective decay rate, velocity, and dispersion coefficients become constants. The laminar flow model shows that a reactive boundary with first order reaction kinetics leads to first order kinetics in the average, cross-sectional bulk flow concentration. The presence of a reactive boundary causes an increase in the effective velocity of the solute plume and a decrease in the effective longitudinal dispersion. It is shown that for laminar flow, the Reynolds number has no impact on the effective transport parameters. Previous studies that have inferred a correlation between the effective decay rate and Reynolds number in the laminar flow regime, are apparently based on the “pre-asymptotic” decay constant and therefore reflect the effects of entrance gradient development.

A turbulent flow model with no boundary reaction was developed, incorporating accurate representations of the velocity profile and turbulent diffusivity in the wall region. The results of this model are compared to Taylor’s classical result of Kau_* (K = 10.1 = constant) for the effective longitudinal dispersion coefficient. The model shows that Taylor’s result does not apply over a wide range of Reynolds numbers and that the coefficient K in fact varies with Reynolds number. The addition of a boundary reaction to the turbulent flow model shows that Reynolds number does have an impact on the effective transport parameters under turbulent conditions. This results from changes in the laminar sublayer thickness.

Acknowledgments

First I'd like to thank Dr. Hari Rajaram for his guidance, advice, and time during this research. I truly appreciate the time he took out of his insanely busy schedule to direct me. I couldn't have had a better advisor.

Thanks to everyone at CADSWES who gave me their support and had to deal with all my CPU poaching. Special thanks to Andrew Gilmore, Janet "Frame Queen" Yowell (who probably deserves some sort of shrine for all the help she gave me), and Edie Zagona for giving me the time to get this done.

No thanks to all my friends for providing endless distractions and being directly responsible for the length of time it took to get this done. But on the other hand, thanks for helping me stay semi-sane during the rough parts.

Finally, thanks to my parents for everything they've done for me basically since birth.

Contents

Introduction 1

1 Background and Thesis Objectives 7
Background 7
Mass Balance Equations 7
Shear Flow Dispersion 8
Taylor Dispersion in Laminar Flow 10
Taylor Dispersion in Turbulent Flow 11
Properties of the Concentration Distribution 14
Effects of a Boundary Reaction 17
Summary of Previous Work on Two-Region Systems with a Boundary Reaction 20
Experiments by Horn and Hempel 20
Modeling Oxygen Consumption by Biofilms in Open Channel Flow 24
Method of Moments Analysis of Transport with Boundary Reactions 25
Limitations of Previous Work 26
Thesis Objectives 26
Analytical Expressions for One-Dimensional Effective Parameters 27
Development of Particle Tracking Model 27
Analysis of Biofilm Characteristics and Diffusive Transport Parameters 28

2 Development of Particle Tracking Models 29
General Particle Tracking Theory: Random Walk Method 29
Laminar Flow Models 31
Transport Within the Bulk Flow 31
Transport and Decay Within the Biofilm 33
Bulk Flow - Biofilm Interface Condition 35
Timestep Restrictions 37
Turbulent Flow Models 39

Mass Transport in the Vicinity of the Pipe Wall 39
Mass Transport in the Turbulent Core 42
Velocity and Diffusivity Profiles 43
Bulk Flow Transport Step Equations 46
Timestep Restrictions 47
System Characterization 48

3 Analytical Solution to Transport in Laminar and Turbulent Flow 50
Laminar Flow Solutions 50
Solution for the Effective Decay Constant 51
Solution for Effective Velocity 55
Solution for the Effective Dispersion Coefficient 56
Turbulent Flow Solution 57

4 Particle Tracking Results and Verification 59
Laminar Flow Results 60
Numerical Issues 64
Dependence of Transport Parameters on Reynolds Number 68
Sensitivity to Porosity and Dbio/D 69
Diffusion Limited Versus Rate Limited Systems 73
Effects of Diffusion Limitation 75
Turbulent Flow Results for a Smooth Pipe 78
Turbulent Transport With No Boundary Reaction 78
Turbulent Transport with a Reactive Biofilm 80
Reynolds Number Dependence 82
Sensitivity to Damkohler Number 85

5 Conclusion 88

References 91

Tables

4.1. Comparison of Simulations to Analytical Results 60
4.2. Discrepancies from Incorrect Numerical Parameters 66
4.3. Mass Transport Parameters for a Range of Reynolds Numbers 68
4.4. Porosity Sensitivity Analysis - Particle Tracking Model 70
4.5. Porosity Sensitivity Analysis - Analytical Model 70
4.6. Sensitivity to Dbio/D - Particle Tracking Model 72
4.7. Sensitivity to Dbio/D - Analytical Model 72
4.8. Porosity Sensitivity - Rate Limited Particle Tracking Model 74
4.9. Porosity Sensitivity - Rate Limited Analytical Solution 74
4.10. Summary of Sensitivity Analysis 75
4.11. Effect of Reynolds Number on Effective Dispersion 79
4.12. Turbulent Flow Results with Biofilm 81
4.13. Dependence of Transport Parameters on Reynolds Number 83

Figures

1.1. Radial Control Volume 8
1.2. Horn and Hempel Results 22
1.3. Entrance Length Region 23
2.1. Dimensionless Velocity Distribution (Wall to Pipe Axis) 44
2.2. Dimensionless Velocity Distribution (Wall Region - Turbulent Core) 44
2.3. Diffusivity/Viscosity Distribution (Wall to Pipe Axis) 45
2.4. Eddy Diffusivity in Wall Region 45
2.5. Diffusivity/Viscosity Distribution (Wall Region - Turbulent Core) 46
4.1. Zeroth Moment Curve 62
4.2. First Moment Curve 63
4.3. Second Moment Curve 64
4.4. Zeroth Moment - Too Few Particles 65
4.5. Second Moment - Too Few Particles 65
4.6. Zeroth Moment - Large Dt 67
4.7. Second Moment - Large Dt 68
4.8. Effective Decay vs. Da 76
4.9. Effective Velocity vs. Da 77
4.10. Effective Dispersion vs. Da 78
4.11. Effect of Reynolds Number on Effective Decay 84
4.12. Effect of Reynolds Number on Effective Dispersion 84
4.13. Effective Decay vs. Damkohler Number 85
4.14. Effective Dispersion vs. Damkohler Number 87

Introduction

Solute transport and reactions are becoming increasingly important topics in the field of Water Resources and Environmental Engineering. In recent years, more emphasis is being placed on water quality than water quantity. In both surface water and groundwater, it is essential to understand the fate and transport of contaminants in natural waters in order to effectively manage water quality. Contaminant transport is a influenced by hydrodynamics as well as the chemistry and biology of the aquatic system. This research will focus on describing the hydrodynamics of transport in the presence of a biological reaction.

Transport within a moving fluid is a result of two processes: advection and diffusion. Advection is solute transport that results from the mean motion of a fluid while diffusion is transport that results from the random motion of the solute molecules. Using a control volume and balancing mass, a partial differential equation can be derived to describe solute transport in a three dimensional system. This equation is the widely known advection-diffusion equation. A reaction term can be added to accommodate a chemical or biological reaction.

The advection-diffusion equation can be modified to describe mass transport in almost any physical system. However for the large-scale, multi-dimensional systems usually studied in engineering applications, the solution of this equation can become

very complicated or even impossible. Simplifying assumptions are invariably required to reduce the complexity of the solution. One approach is to reduce the dimensionality of the equations and describe the system in terms of “effective” parameters. The effective parameters serve to capture the effects of multiple dimensions so a system can be described in a single dimension. The goal of this thesis is to quantify the effective transport parameters for a circular pipe, with and without a reactive biofilm, under laminar and turbulent flow conditions.

The three dimensional advection-diffusion equation for concentration in a circular pipe with a boundary reaction can be reduced to one dimension (along the axis of the pipe) in terms of the cross-sectional concentration. The solution of this equation involves an effective decay constant, an effective velocity, and an effective dispersion coefficient (termed the effective transport parameters). When describing the system in multiple dimensions, the decay constant used in the advection-diffusion equation would be the decay constant in the reactive biofilm. Solute would decay according to this decay constant only when it is located in the biofilm region of the pipe. However, the effective decay rate used to describe the system with one dimension, represents the overall reduction of the cross sectional average concentration due to the presence of a boundary reaction. It is thus likely to be much smaller than the decay rate within the biofilm, and should also reflect the influence of diffusive exchange between the bulk flow and biofilm. The effective velocity represents the longitudinal (axial) velocity of the center of mass of the solute plume and the effective dispersion coefficient represents the spread of the solute plume in the longitudinal direction.

Horn and Hempel (1995) attempted to quantify the effective decay coefficient for a short tube reactor under laminar flow conditions. The study used a numerical model, calibrated with experimental data, to quantify the effects of a reactive biofilm on bulk flow mass transfer. The goal of the study was to modify an existing mass transfer equation, for a pipe with no biofilm, to include the effects of a boundary reaction.

While the mass transfer coefficient empirically developed by Horn and Hempel matched their experimental data quite well, it appears that their interpretation of the mechanisms controlling mass transfer and reaction is incorrect. In particular, they propose a Reynolds number dependence of the effective decay rate, even though all their experiments were carried out in the laminar flow regime. We believe that the empirical relationships developed by Horn and Hempel are reactor-specific, in other words, they can only model the mass transfer coefficient for their reactor and are not generalizable to all coated biofilm pipe reactors. Due to the short length of their pipe reactor, it appears that their results reflect the influence of laminar flow that is not yet fully developed (for the higher flow rate cases) and "pre-asymptotic transport", wherein the diffusive interactions between the pipe and biofilm have not reached an equilibrium condition. Cox (1997) showed that under these conditions, representation of one-dimensional transport in terms of an effective decay constant or mass transfer coefficient is not valid. In fact, for fully developed laminar flow, after diffusive equilibrium between the biofilm and bulk flow is achieved, Cox (1997) showed that the effective decay constant is independent of Reynolds number.

Cox (1997) used a method of moments approach to analytically solve the one-dimensional advection-diffusion equation for a circular pipe with a reactive boundary under laminar flow conditions. This resulted in analytical expressions for the effective decay, effective velocity, and effective dispersion coefficient. The results were verified with a finite difference numerical solution of the multi-dimensional advection-diffusion equation. The analytical expressions were successful in demonstrating the effects of a reactive biofilm on the effective transport coefficients. However the models were limited to laminar flow conditions and were subject to inaccuracies under certain conditions. Also, the numerical model was subject to considerable numerical dispersion. The research performed in this thesis aims to reproduce Cox's results with a more accurate and flexible modeling approach and to extend these models to include turbu-

lent flow conditions.

A particle tracking model was constructed to simulate mass transport in a circular pipe. The theory behind particle tracking models involves statistics and the random walk method of modeling. Basically the model uses a large number of particles which move independently of one another. Each particle is subject to random motion but is restricted so that the average motion of all the particles meets certain statistical requirements. The idea is that each particle represents a solute molecule that moves about due to Brownian motion. Depending on the location of the particle in the system, it may also be subject to advection due to a velocity field or large scale random motion caused by turbulence. The velocity field, degree of random particle motion, and statistical nature of the model can be adjusted to accommodate various physical systems.

Since particle tracking models are based on statistics and do not involve a solution to the advection-diffusion equation, they can be used to describe highly complex physical systems that could not be modelled otherwise. The application of particle tracking models to the field of groundwater hydrology is highly relevant. They are currently used to describe contaminant transport in porous media and fractured flow systems. However, the particle tracking model developed in this research is designed to specifically describe solute transport in a circular pipe. The laminar flow results obtained from the particle tracking model coincide with Cox's research and give valuable insight to the relationship between biofilm characteristics and the effective transport parameters. The zeroth, first and second mass moments of the solute plume are used to determine the transport parameters. In general, as the reactive properties of the biofilm increase, the effective decay rate increases and the effective dispersion decreases.

There are two important aspects to the development of the turbulent flow model. The first deals with the velocity and diffusivity profiles used in the model. (In

turbulent flow radial transport occurs as a result of turbulent eddies as opposed to molecular diffusion. The term used to describe this form of radial transport is the eddy diffusivity and it varies with the radial location in the pipe.) A pipe experiencing turbulent flow conditions is comprised of two distinct regions of flow; the turbulent core and the laminar boundary layer. The turbulent core makes up the majority of the pipe cross section and is characterized by large rotational eddies and high flow velocities. The laminar boundary layer exists very close to the pipe wall. In this region the turbulent eddies dissipate and viscous forces tend to dominate the flow field much like laminar flow. The velocity and diffusivity profiles in the turbulent core are well defined and have been confirmed by experimentation; however in the wall region this is not the case. There have been several attempts to develop velocity and diffusivity profiles for the laminar sublayer that are continuous with the respective profiles in the turbulent core. While there is some debate about the exact nature of the wall region, one of the more well known studies was used to develop the velocity and diffusivity profiles in this research.

While there has been considerable research in describing the wall region of a pipe in turbulent flow, no attempt has been made at describing the nature of transport in the entire system since Taylor's classical work (Taylor, 1954). Taylor attempted to quantify the effective dispersion coefficient in a circular pipe under turbulent flow conditions. At that time, the universal velocity profile for the turbulent core had not been developed and no extensive research had been performed on the velocity and diffusivity in the wall region. For the turbulent core, a velocity profile which was very near to the universal profile was used. A linear velocity profile was used in the wall region. Given these profiles, Taylor showed that the effective dispersion coefficient can be expressed as $10.1au_*$ where a is the pipe radius and u_* is the shear velocity. The models developed in this research using the more recent expressions for velocity in the wall region show that the effective dispersion coefficient varies with Reynolds number

and hence the “constant” 10.1 is not really constant. This is an important discovery since Taylor’s result has been accepted since 1954 and additional research on the topic has not been performed since then.

The second aspect of the turbulent flow models involves the addition of a reactive biofilm. There is no documentation of any research attempting to describe this system. The model results show that a reactive biofilm has similar effects on the effective transport coefficients in a turbulent system as that in a laminar flow system. One important difference, however, is that in laminar flow the effective decay constant does not vary with Reynolds number while in turbulent flow it does.

In summary, the particle tracking models developed in this research successfully quantify the effective transport parameters for a circular pipe with a boundary reaction for both laminar and turbulent flow. The laminar flow models produce results that match with Cox’s analytical and numerical results. The non-reactive turbulent flow models show that for the more recent velocity profiles in the turbulent core and the wall region, the effective dispersion coefficient varies with Reynolds number and is therefore inconsistent with Taylor’s result. This calls for additional physical experimentation of dispersion in turbulent pipe flow for a wide range of Reynolds numbers.

Chapter 1

Background and Thesis Objectives

1.1 Background

Mass Balance Equations

Transport within a moving fluid essentially takes place as a result of two mechanisms; advection and diffusion. Advection is defined as the transport of solute due to the mean motion of the fluid. Diffusion, on the other hand, is transport due to the random motion (brownian motion) of solute molecules. Using a control volume approach and performing a mass balance, the following equation can be derived to describe the advection-diffusion system:

$$n\frac{\partial C}{\partial t} + nu(y,z)\frac{\partial C}{\partial x} - \frac{\partial}{\partial x}\left(nD_x\frac{\partial C}{\partial x}\right) - \frac{\partial}{\partial y}\left(nD_y\frac{\partial C}{\partial y}\right) - \frac{\partial}{\partial z}\left(nD_z\frac{\partial C}{\partial z}\right) = 0 \qquad \text{Eq. 1.1}$$

where x is the longitudinal direction, y and z are perpendicular to the longitudinal direction, t is time, $u(y,z)$ is the velocity in the x direction as a function of y and z, n is the porosity of the medium, and D_x, D_y, and D_z are the diffusion coefficients in the respective directions. Equation 1.1 is commonly referred to as the "advection-diffusion equation."

Due to radial symmetry, flow within a circular pipe can be described with only two space variables using a radial coordinate system. In radial coordinates, Equation

1.1 reduces to:

$$n\frac{\partial C}{\partial t} + nu(r)\frac{\partial C}{\partial x} - \frac{1}{r}\frac{\partial}{\partial r}\left(nrD_r\frac{\partial C}{\partial r}\right) - \frac{\partial}{\partial x}\left(nD_x\frac{\partial C}{\partial x}\right) = 0 \qquad \text{Eq. 1.2}$$

where r is the radial position. Figure 1.1 illustrates the control volume for the radial coordinate system.

Figure 1.1: Radial Control Volume

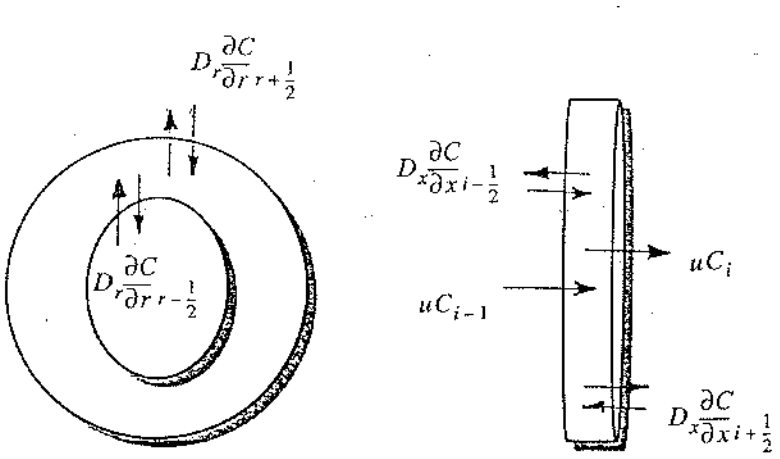

Equation 1.2 can be solved analytically or numerically to determine the concentration as a function of time, the radial position, and longitudinal position. This solution is not easily obtained and is sometimes unnecessary. A more useful approach would be to develop an equivalent one-dimensional “effective transport” equation.

Shear Flow Dispersion

Shear flows involve velocity distributions perpendicular to the flow direction. Often, these velocity distributions do not change along the flow direction. An example of such flow is laminar flow in a straight, closed conduit with a constant cross section. Common to all shear flows is that solute spreading in the direction of flow is dominated by the velocity profile in the cross section (Fischer, 1979). For example, if a par-

ticle was located near the wall of a pipe and another was located in the center of the pipe, their rate of spreading (with respect to each other) due to velocity differences would greatly exceed that of molecular diffusion. However, given enough time, a solute particle's random motion, due to molecular diffusion, will cause it to sample the entire velocity profile. Therefore, eventually, the time-averaged velocity of any particle will equal the cross sectionally averaged velocity in the pipe (Taylor, 1953). However, the rate of separation of particles will still be much greater than if all particles were travelling at the same advective velocity. This enhanced spreading due to the interaction between the velocity profile and transverse diffusion is commonly referred to as dispersion.

Taylor (1953) showed that an effective longitudinal dispersion coefficient can be used to represent the dispersive effects of both transverse diffusion and the variation of the velocity profile. This assumption has been shown to be valid only after a "development length" or "development time", whereby the effective longitudinal coefficient has reached an asymptotic value (Taylor, 1953). Using this assumption, and averaging the concentration and velocity of the entire cross section, a one dimensional, effective advection-dispersion equation can be derived:

$$\frac{\partial}{\partial t}\overline{C} + \bar{u}\frac{\partial}{\partial x}\overline{C} - D^{*}\frac{\partial^{2}}{\partial x^{2}}\overline{C} = 0 \qquad \text{Eq. 1.3}$$

where $\overline{C}$ is the cross-section average concentration, $\bar{u}$ is the average velocity, and D^{*} is the effective longitudinal dispersion coefficient.

While Equation 1.3 is useful for describing the effective one-dimensional parameters of a system, it is not always applicable. Initially, the distribution of solute has a major impact on local concentrations and dispersion. Advective dispersion and molecular diffusion have yet to reach a balance so an effective dispersion coefficient cannot be used. In order to model this process, it is necessary to use Equation 1.2.

After a long enough development time however, each solute particle has sampled the entire velocity field several times and the initial distribution of solute ceases to have an impact on dispersion. The velocity of each solute particle is independent of its initial velocity. Advective and diffusive transport have reach an equilibrium and the effective dispersion coefficient has reached an asymptotic value. Also, the solute concentration is uniformly distributed across any given cross section. At this point, a pseudo-steady state condition has been established in a coordinate system moving at $\bar{u}$ and Equation 1.3 can be used to model the process.

Taylor Dispersion in Laminar Flow

At low Reynolds numbers, when viscous forces dominate inertial forces, flow is laminar. The velocity at any given radial location is constant and the instantaneous velocity profile is smooth because there are no temporal velocity fluctuations due to turbulence. Therefore, lateral transport of solute occurs by molecular diffusion only. As the solute moves through various velocity streamlines, it is transported in the longitudinal direction by advection. Since, at any given time, solute exists throughout the velocity field, solute separation will occur due to velocity differences (as discussed above). Molecular diffusion also occurs in the longitudinal direction; however, it is almost negligible when compared to solute separation and transport by advection. In a circular pipe, the velocity profile for laminar flow can be described by the familiar parabolic profile:

$$u(r) = u_{max} \cdot \left(1 - \frac{r^2}{a^2}\right) \qquad \text{Eq. 1.4}$$

where u(r) is the velocity at radial position, r, u_{max} is the maximum velocity (at the center of the pipe), and a is the radius of the pipe. If Equation 1.4 is integrated over the radius of the pipe and divided by the cross sectional area of the pipe, the mean velocity

is calculate as one half of the centerline velocity. Taylor (1953) derived an analytical expression for the asymptotic value of the effective longitudinal dispersion coefficient in laminar flow:

$$D^* = \frac{a^2 u_{max}^2}{192 D} \qquad \text{Eq. 1.5}$$

or

$$D^* = \frac{a^2 \bar{u}^2}{48 D} \qquad \text{Eq. 1.6}$$

where D^* is the effective longitudinal dispersion coefficient and $\bar{u}$ is the average cross sectional velocity. The previous two equations have been verified through laboratory experimentation and will be used to confirm the models developed in this thesis.

Taylor Dispersion in Turbulent Flow

In turbulent flow, inertial forces dominate viscous forces. The instantaneous velocity profile is not a smooth curve and the velocity at a given radial position fluctuates with time. Statistical analysis can be used to determined a time-averaged velocity profile. This is the mean value of the velocity over a time scale which is much greater than the time scale of the individual fluctuations. In the equations and discussion that follow, the velocities referred to are always the time-averaged velocities.

Extensive experimentation has shown that the turbulent velocity profile is logarithmic in the radial direction except near the walls of the pipe. A velocity profile that matches the experimental results can be derive using the Prandlt mixing length theory (Wilkes, 1999). Assume now that the variable *y* is the distance from the pipe wall (y = a - r). Prandlt's hypothesis assumes that there is a direct proportionality between the mixing length, *l*, and the distance from the wall, *y.* Also assume a constant shear stress,

τ, which is equal to its value, τ_w, at the wall. This is true only for a small interval near the pipe wall.

$$l = ky \qquad \text{Eq. 1.7}$$

$$\tau = \tau_w \qquad \text{Eq. 1.8}$$

where k is a constant. In actuality, Equation 1.7 and Equation 1.8 are overestimates for both l and τ. However, both overestimates tend to cancel each other out and give an excellent result for the turbulent velocity profile (Wilkes, 1999). Mixing length theory gives the following relationship:

$$\tau = \rho l^2 \left(\frac{du}{dy}\right)^2 \qquad \text{Eq. 1.9}$$

where u is the time-averaged velocity as a function of y. du/dy is recognized as positive since the time-averaged velocity increases as the distance from the wall increases. Using Equation 1.7 and Equation 1.8, Equation 1.9 can be rewritten as:

$$\tau_w = \rho k^2 y^2 \left(\frac{du}{dy}\right)^2 \qquad \text{Eq. 1.10}$$

Equation 1.10 integrates to:

$$u = \frac{1}{k}\sqrt{\frac{\tau_w}{\rho}} \ln y + c \qquad \text{Eq. 1.11}$$

where c is a constant of integration.

Equation 1.11 is used to develop what is known as the universal velocity profile for turbulent flow in a smooth pipe. It is first useful to define some non-dimensional

parameters. The term $\sqrt{\tau_w/\rho}$ is commonly known as the friction velocity or shear velocity, u_*. Using this definition, a dimensionless variables for y and u can be defined as:

$$y^+ = \frac{yu_*}{\upsilon} \qquad \text{Eq. 1.12}$$

$$u^+ = \frac{u}{u_*} \qquad \text{Eq. 1.13}$$

where υ is the kinematic viscosity. Equation 1.11 can now be rewritten as:

$$u^+ = A + B\ln y^+ \qquad \text{Eq. 1.14}$$

where A is the constant of integration and B is $1/k$. Experimentation has shown the constants to be 5.5 and 2.5, respectively. The final form of the universal velocity profile is shown below:

$$u^+ = 5.5 + 2.5\ln y^+ \qquad \text{Eq. 1.15}$$

The universal velocity profile matches experimental results in the turbulent core, however, it does not hold in the wall region because it gives an ever-increasing negative velocity and an ever-increasing velocity gradient as y approaches zero. The no-slip condition for fluids in as pipe requires that velocity is zero when y is zero. There is more than one way to describe the velocity variations in the wall region. This will be discussed further during the development of the models used to describe this system.

In turbulent flow in a pipe, relatively large rotational eddies are formed in the region of high shear near the wall which degenerate into progressively smaller eddies, dissipating energy into heat by the action of viscosity (Wilkes, 1999). The motion of

these eddies is responsible for the transfer of solute in the radial direction. The coefficient of lateral transport must therefore include the effects of eddy diffusivity as well molecular diffusion in order to accurately describe lateral transport. This coefficient, termed the eddy molecular diffusivity, simply replaces the molecular diffusion coefficient in the equations used to describe dispersion in laminar flow. Using Reynold's analogy, which assumes that the mixing coefficients for momentum and mass are the same, the eddy molecular diffusivity can be expressed as:

$$\varepsilon = -\frac{m}{\partial C/\partial r} = -\frac{\tau}{\rho\frac{\partial u}{\partial r}} - \upsilon = -\frac{\tau_w(r/a)}{\rho\frac{\partial u}{\partial r}} - \upsilon \qquad \text{Eq. 1.16}$$

where m is the rate of radial transfer of matter of concentration C.

The extension of the laminar flow analysis to turbulent flow involves using the universal velocity profile (instead of the laminar flow profile) and the eddy molecular diffusivity (instead of the molecular diffusion coefficient). The conclusions reached about the use of the one dimensional advection-dispersion equation (described previously) remain unchanged (Fischer, 1979). The only significant difference is that the eddy molecular diffusivity varies as a function radial position. Therefore, Taylor was able to derive an expression for the asymptotic value of the effective longitudinal dispersion coefficient in turbulent flow:

$$D^* = 10.1 a u_* \qquad \text{Eq. 1.17}$$

Properties of the Concentration Distribution

In 1956, Aris developed an alternative method for characterizing effective transport parameters (Aris, 1956). Commonly referred to as the method of moments, Aris used various moments of the concentration distribution to determine properties of the advection-dispersion system. The p^{th} concentration moment is defined by the fol-

lowing equation:

$$C_p = \int_{-\infty}^{+\infty} x^p C(x, r, t)dx \qquad \text{Eq. 1.18}$$

where x is the longitudinal position and $C(x,r,t)$ is the concentration with respect to longitudinal position, radial position and time.

Equation 1.18 is used to compute the concentration moment at a given radial position, r. This is not very useful for determining overall effective parameters. The concentration moment must be integrated over the entire cross section to include all radial positions. Equation 1.18 then becomes:

$$M_p(t) = \int_0^a 2\pi r \int_{-\infty}^{+\infty} x^p C(x, r, t)dxdr \qquad \text{Eq. 1.19}$$

where M_p is the cross sectional average of C_p as a function of time, and a is the radius of the pipe. It is apparent that the zeroth moment, $M_0(t)$, represents the total mass in the system at any time t:

$$M_0(t) = \int_0^a 2\pi r \int_{-\infty}^{+\infty} C(x, r, t)dxdr \qquad \text{Eq. 1.20}$$

Therefore, the one dimensional effective decay coefficient, k^*, can be expressed as:

$$k^* = \frac{dM_0/dt}{M_0} \qquad \text{Eq. 1.21}$$

This comes from the definition of first order kinetics: $dM/dt = k^* M_0$. For non-reactive transport as described by Equation 1.1 and Equation 1.2, $k^* = 0$ and M_0 is a constant equal to the initial mass introduced to the system.

The first moment, M_1, is defined as:

$$M_1(t) = \int_0^a 2\pi r \int_{-\infty}^{+\infty} xC(x, r, t)dxdr \qquad \text{Eq. 1.22}$$

The first moment represents a weighted summation of longitudinal positions over the entire system volume. If this weighted sum is divided by the entire mass in the system, the result is a weighted average of longitudinal positions. This is equivalent to the center of mass in the system, defined as:

$$\overline{X}(t) = \frac{M_1}{M_0} \qquad \text{Eq. 1.23}$$

where $\overline{X}(t)$ is the mass centroid as a function of time. The change in centroid position with respect to time represents the effective velocity of the center of mass of the solute plume:

$$U_{eff} = \frac{d(M_1/M_0)}{dt} = \frac{d\overline{X}}{dt} \qquad \text{Eq. 1.24}$$

In a pipe with no reaction, U_{eff} is equal to the mean velocity of the fluid.

The second moment of mass is defined as:

$$M_2(t) = \int_0^a 2\pi r \int_{-\infty}^{+\infty} x^2 C(x, r, t)dxdr \qquad \text{Eq. 1.25}$$

It can be shown that the longitudinal variance of the solute plume is expressed as:

$$\sigma^2 = \frac{M_2}{M_0} - \overline{X}^2(t) \qquad \text{Eq. 1.26}$$

The rate of change of the variance represents the rate of change of the solute spread in the longitudinal direction. This has been shown to be proportional to the effective one dimensional dispersion coefficient (Fischer, 1979).

$$\frac{d\sigma^2}{dt} = 2D^* \qquad \text{Eq. 1.27}$$

In general, a non-reactive solute plume will have a gaussian distribution once the initial development time has elapsed. If a coordinate system that moves with the mean velocity of the flow is adopted, the mean of the solute distribution is zero and the variance is: $\sigma^2 = 2D^* t$. However, as discussed in the following section, this is not necessarily the case if a boundary reaction exists.

Effects of a Boundary Reaction

In context of biological treatment of wastewater, biofilm reactors with simplified geometries have been studied. The objective of these studies are to quantify effective reaction rates and other effective transport parameters. Among the systems studied, are biofilm coated pipe reactors (Horn and Hempel, 1995) and (Cox, 1997). Dissolved oxygen and substrates that are biodegradable can be consumed within the biofilm. This can be modeled by including a reaction term in the two dimensional equation (Equation 1.2) that is active only for the boundary region.

$$n\frac{\partial C_i}{\partial t} + nu(r)\frac{\partial C_i}{\partial x} - \frac{1}{r}\frac{\partial}{\partial r}\left(nD_{ri}\frac{\partial C_i}{\partial r}\right) - \frac{\partial}{\partial x}\left(nD_{xi}\frac{\partial C_i}{\partial x}\right) + rxn = 0, i = 1, 2 \qquad \text{Eq. 1.28}$$

where $i = 1$ refers to the bulk flow and $i = 2$ refers to the biofilm region. In the bulk flow region, the reaction term, *rxn*, is equal to zero ant the porosity is one. Two boundary conditions are used to define the system at the bulk flow - biofilm interface: equal concentration at the interface

$$C_1 = C_2, at\ r = \text{interface} \qquad \text{Eq. 1.29}$$

and equal flux at the interface

$$D_{r1}\frac{\partial C_1}{\partial r} = nD_{r2}\frac{\partial C_2}{\partial r}, \text{ at } r = \text{interface} \qquad \text{Eq. 1.30}$$

The reaction term, *rxn*, may be zero order, first order, or non-linear. In this thesis, non-linear reactions are not considered. A zero order reaction term has the form $+nk$, where n is the porosity and k is the decay constant. A reaction of this type occurs at a constant rate regardless of the concentration. A first order reaction is represented by the term $+nkC_2$ where C_2 is the solute concentration in the biofilm. This takes the form of an exponential decay of solute in the reactive region.

In a laminar flow system, transport of solute to the reactive boundary takes place by diffusion only. Therefore, transport into the biofilm is governed by the molecular diffusion coefficient and the concentration gradient that exists across the biofilm-bulk flow interface (according to Fick's Law) (Cox, 1997). Once the solute reaches the boundary and enters the biofilm, it then decays according to the appropriate reaction type. Diffusive transport may take place within the biofilm allowing the solute to re-enter the bulk flow. Advection of solute usually does not occur within the biofilm coating on the pipe walls and will not be considered in this thesis.

In a turbulent flow system, there are two regions involved with transport in the radial or transverse directions. Boundary layer theory dictates that a laminar sublayer exists very close to the pipe wall where viscous forces dominate inertial forces. Turbulent eddies do not exist in the laminar sublayer so diffusion to the biofilm region is Fickian in nature and therefore controlled by the molecular diffusion coefficient and the concentration gradient across the sublayer. In the turbulent core, radial transport is dominated by the turbulent eddies. The eddy diffusivity control transport to the laminar sublayer.

In order to incorporate a reactive biofilm boundary in the one-dimensional transport equation, an effective decay term can be added.

$$\frac{\partial}{\partial t}\overline{C} + U_{eff}\frac{\partial}{\partial x}\overline{C} - D^{*}\frac{\partial^{2}}{\partial x^{2}}\overline{C} + k^{*}\overline{C} = 0 \qquad \text{Eq. 1.31}$$

where U_{eff} is the effective velocity, D^{*} is the effective dispersion coefficient, and k^{*} is the effective decay coefficient. The decay term represents the decay of the cross sectional average concentration. The effective decay rate will be smaller than the decay rate in the biofilm because decay is confined only to the boundary region. The effective decay term will reflect the balance that is achieved between the diffusive transport from the bulk flow into the active boundary regions and the concentration decay within these regions (Cox, 1997). Initially, diffusive processes will dominate as the solute is transported to the boundary region. However, once the initial boundary gradients have been established and the conditions for one-dimensional representation have been achieved, a constant term can be used in the mass balance for the bulk flow. Cox, in 1997, showed that for laminar flow the effective decay term can be limited by either diffusion or kinetics, depending upon the magnitude of the decay coefficient in the biofilm in comparison to the molecular diffusion coefficient. In this thesis, the investigation into the nature of the effective decay term will be continued for laminar flow systems and extended to turbulent flow.

The one dimensional effective velocity, U_{eff}, and dispersion, D^{*}, coefficients will be affected by the existence of a boundary reaction. The effective velocity of the centroid of the solute plume may or may not travel at the mean speed of flow. Also, the concentration distribution may not be a normal, symmetrical Gaussian curve. The distribution will still be Gaussian in nature, however, there may be a degree of skewness and the variance will be different from that of a solute plume with no boundary reaction. The existence of a reactive boundary will cause the cross sectional concentration distribution to be non-uniform. More solute will exist in the center of the pipe because solute near the pipe wall is subject to decay. This will cause the effective velocity of the solute plume to increase because more mass exists in regions of higher velocity.

For the same reason, the effective dispersion coefficient will decrease because less solute will exist in the regions of highest shear (near the wall). In other words, more solute will exist in the center of the pipe where the velocity variations are less severe. Therefore, there will be decreased longitudinal separation among the solute particles. When using the one-dimensional transport equation with a boundary reaction these parameters need to be adjusted accordingly. Methods of characterizing the effective one-dimensional parameters will be discussed later in this thesis.

1.2 Summary of Previous Work on Two-Region Systems with a Boundary Reaction

Following is a summary of the previous work involving the characterization of bulk flow - biofilm systems. Also, included is some work dealing with open channel flow with a reactive bed. The problem of describing mass transport in a system with a reactive boundary has not been extensively studied in the field of water resources engineering. Most of the background theory is taken from mass transport studies in the field of chemical engineering or analogous theories in heat transport. Therefore, a well established background to this research does not exist. The following studies are discussed to provide a frame of reference and to demonstrate how similar research problems have been approached in the past.

Experiments by Horn and Hempel

Horn and Hempel (1995) performed a series of experiments aimed at evaluating the mass transfer coefficients at a bulk flow - biofilm interface. This was done by modifying an existing expression for radial mass transfer in a circular pipe with no biofilm to reflect the effects of a biofilm coating. A numerical model was used to calculate concentration profiles and was calibrated by adjusting the mass transfer coefficient to match the measured profiles. In this way, mass transfer coefficients were estimated for various flow rates within the laminar flow regime.

The Sherwood number, *Sh*, is a dimensionless number used to describe mass transfer for laminar flow in tube reactors without biofilms:

$$Sh = 2Re^{1/2}Sc^{1/2}(d/L)^{1/2} \qquad \text{Eq. 1.32}$$

where *Re* is the Reynold's number, *Sc* is the Schmidt number (momentum transfer / mass transfer), *d* is the tube diameter, and *L* is the tube length. The length of the tube reactor used in the experiments and in the models was constant at 163 cm. The diameter of the tube was 1.6 cm and the biofilm thickness was 0.035 cm on average. The numerical model used to estimate mass transfer was based on the following equation:

$$D\frac{\partial C}{\partial r} = \beta(C_B - C_F) \qquad \text{Eq. 1.33}$$

where C_B and C_F are the concentrations in the bulk flow and at the biofilm surface, respectively, and β is the mass transfer coefficient. Mass transfer coefficients were estimated for various flow rates within a range of Reynold's numbers from 532 - 1894. The numerical/experimental mass transfer coefficients were about one order of magnitude less than those given by Equation 1.32. It was surmised by Horn and Hempel that this discrepancy was due to the fact that Equation 1.32 did not account for a boundary reaction and the boundary layer close to the wall. Therefore it was modified in the following manner to better fit the experimental data:

$$Sh = 2Re^{1/2}Sc^{1/2}(d/L)^{1/2}(1 + 0.0021Re) \qquad \text{Eq. 1.34}$$

Figure 1.2 shows the experimental results in relation to Equation 1.32 and Equation 1.34.

Figure 1.2: Horn and Hempel Results

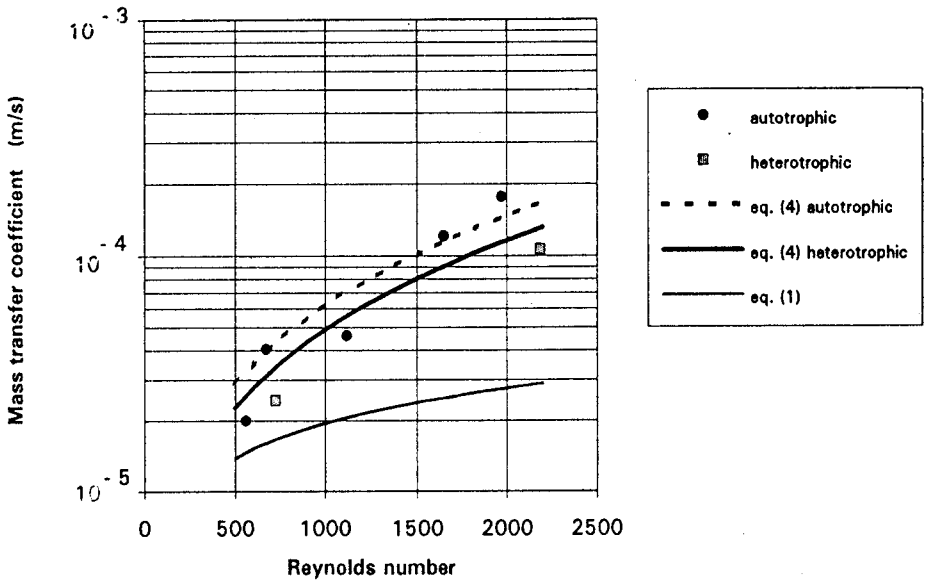

In Figure 1.2, “equation 1” represents Equation 1.32 and “equation 4” represents Equation 1.34. It is obvious that Equation 1.34 fits the data much better that Equation 1.32. However, it also obvious that the mass transfer coefficient varies with Reynold’s number. According to the theory of Taylor dispersion in laminar flow (discussed previously), the effective mass transfer coefficient does not depend on *Re.* (Incidentally, in turbulent flow, the effective one-dimensional mass transfer coefficient is dependent on Reynold’s number. As Reynold’s number increases turbulence increases and the thickness of the laminar sublayer decreases, thereby increasing mass transfer to the biofilm region. This is discussed in greater detail in later chapters.) The tube reactor used in the Horn and Hempel experiments was relatively short (163 cm). At the lowest Reynold’s number used in the experiments (534), the travel time in the pipe would be about 50 seconds. According to the theory of shear flow dispersion, an initial development time is required before the effective mass transfer coefficient reaches a constant, asymptotic value. The following equation can be used for estimating the initial development length for laminar flow (Cox, 1997):

$$\frac{L}{d} = 0.05 ReSc \qquad \text{Eq. 1.35}$$

where L is the development length, Re is the Reynold's number, and Sc is the Schmidt number. For a Reynold's number of 534, this results in a development length of 20000 cm and a development time of about 6000 s. Therefore, the development time is never reached in the Horn and Hempel experiments. The mass transfer coefficient has not reached an asymptotic value and the assumption of a constant value for the mass transfer coefficient is not valid. Horn and Hempel's interpretation of their data using a mass transfer coefficient dependent on Reynolds number is therefore inappropriate. They are actually fitting the pre-asymptotic behavior of the effective reaction rate using a Reynolds number dependence.

In addition to the initial development time required to achieve effective one-dimensional transport, an entrance development length is required before fully laminar flow conditions can be established.

Figure 1.3: Entrance Length Region

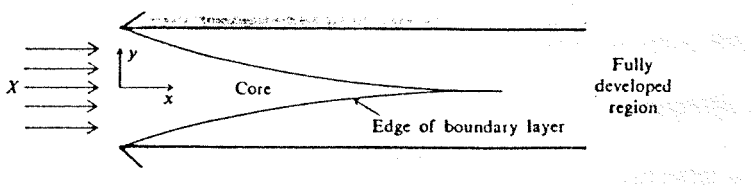

As shown in Figure 1.3 a laminar boundary layer grows in thickness from the pipe walls to the center of the pipe. A turbulent core penetrates the laminar boundary layer until fully laminar conditions are reached. The length of this turbulent core is the entrance development length. Within the turbulent core, radial velocities and turbulent eddies contribute to mass transport. Therefore, the molecular diffusion coefficient cannot be used to describe radial transport in this region. The following expression can be used to estimate the entrance length (Cox, 1997):

$$L_e = 0.0575 Re \cdot d \qquad \text{Eq. 1.36}$$

For the range of Reynold's numbers used in the Horn and Hempel experiment, entrance lengths vary from 50 - 100 cm. Therefore, for higher Reynold's numbers, fully laminar conditions are not even established within the tube reactor.

It is obvious that the assumption of a constant mass transport coefficient in the Horn and Hempel tube reactor is invalid. Effective one-dimensional conditions are never established and in some cases fully laminar conditions are not even established. Therefore, it is assumed that the mass transfer coefficients calculated by Equation 1.32 and Equation 1.34 represent average transfer coefficients for the length of the reactor. The values of the coefficients would be dependent upon both the degree of penetration of the turbulent core and the travel time through the pipe. Thus a direct relationship between the Reynold's number and average transfer coefficient would exist. It is assumed that Equation 1.32 and Equation 1.34 were developed for short tube reactors with laminar flow, where the reactor lengths are of the same scale as the entrance lengths. Therefore, their findings are applicable on a reactor specific basis only.

Modeling Oxygen Consumption by Biofilms in Open Channel Flow

In 1994, S. Li and G.H. Chen developed a mathematical model to predict the removal of dissolved organic substances and the consumption of dissolved oxygen by attached, benthic biofilms in an open channel flow (Li and Chen, 1994). The conventional Streeter-Phelps equation was combined with the biofilm equations resulting in a system of equations that could be solved numerically.

The model assumed that transfer of matter occurred from a bulk flow region, through a diffusion layer (laminar sublayer), and into the biofilm where reaction took place. Two dimensional mass balance equations were coupled for each of the regions and included the effects of molecular diffusion through the diffusion layer, mean velocity in the bulk flow, reaeration in the bulk flow, and Dual Monod reaction kinetics in the biofilm. The resulting non-linear system was solved by a trial and error approach

to a finite difference numerical model.

The results of the model show that the effects of a biofilm have a significant influence on organic removal and oxygen consumption. The traditional Streeter-Phelps equation is based on the removal rates of the suspended biomass which are usually determined from BOD bottle tests. However the modified Streeter-Phelps model shows that the removal rates caused by the biofilm are greater than those resulting from suspended biomass. Some studies have shown that streambed biomass accounts for 90% of the oxygen consumption (Li and Chen, 1994). Li and Chen also studied the effects of bulk flow velocity on the diffusive layer thickness and benthic uptake. In general an increase in velocity leads to a decrease in thickness of the diffusive layer. As diffusive layer thickness decreases, benthic uptake becomes less diffusion limited so uptake should increase. However, as the bulk flow velocity increases, contact time with the biofilm decreases and so uptake should decrease. The overall result of the experiments suggests that contact time is more significant than the diffusive layer thickness. Another finding made by Li and Chen is that uptake increases as biofilm thickness increases up to a certain point. Beyond a certain thickness, diffusion limitations dominate and the uptake reaches a constant value. Both the net effects of bulk flow velocity and biofilm thickness will be explored in this thesis.

Method of Moments Analysis of Transport with Boundary Reactions

Tim Cox (1997) quantified the effects of boundary reactions on bulk flow solute transport parameters in a biofilm-coated pipe under laminar flow conditions. The emphasis of the research was to use both numerical and analytical approaches to establish relationships between effective bulk flow transport parameters and biofilm properties. Also explored was the time scale associated with the development region of transport.

Using Aris' method of moments approach, analytical expressions were devel-

oped for the effective one dimensional decay coefficient, the effective velocity, and the effective dispersion coefficient. These expression will be described in detail in a later chapter and will be used to verify models developed in this research. The numerical models were based on a finite-difference approach for solving the advection-dispersion equation. These results were used to verify the analytical results. The numerical model was very successful in verifying the analytical expressions for effective decay and effective velocity. However there was some discrepancy in the effective dispersion coefficients. It is believed that this is a result of numerical dispersion commonly encountered in finite-difference models.

Limitations of Previous Work

Of the previous work just described, only Tim Cox attempted to quantify the effects of a boundary reaction on the bulk flow transport parameters. However, his work was limited to laminar flow conditions. Also, the numerical model used in his research had inaccuracies due to numerical dispersion.

As discussed previously, Horn and Hempel's experiments were unable to describe the asymptotic, effective transport parameters. Their work was limited to a tube reactor that was not long enough to establish conditions that could be described with one dimensional parameters. Their findings seem to be applicable on a reactor specific basis only. While Li and Chen were successful in describing a two-region system with boundary reactions. Their work was applied to open channel flow and therefore, is not directly related to the research in this thesis.

1.3 Thesis Objectives

The background material just described will be used as a basis to characterize the one-dimensional transport parameters for a laminar and turbulent flow system. This will first be done for a circular pipe with no biofilm to reproduce the results discussed previously. Tim Cox, in 1997, extended this theory to a circular pipe with a

reactive biofilm under laminar flow conditions. A particle tracking model will be used to reproduce his results and then extend the analysis further to describe a turbulent flow system with a reactive biofilm. In this way the problem of numerical dispersion, as seen in Tim Cox's work, will be avoided.

The main objective of this work is to show the relationship between various biofilm characteristics and the effective bulk flow and transport parameters in laminar and turbulent pipe flow. A particle tracking model is used to simulate 3-dimensional transport and calculate the resulting effective parameters. These are verified with analytical results. The particle tracking model is also used to characterize the transport system in the development stages, before the effective parameters reach an asymptotic value. The following specific tasks are undertaken to accomplish the stated objectives.

Analytical Expressions for One-Dimensional Effective Parameters

Aris' method of moments procedure will be applied to a circular pipe with a reactive biofilm. Only a first order reaction rate will be considered in the derivation of the analytical expressions. Analytical expressions will be developed for the effective one-dimensional decay rate, velocity, and dispersion coefficient. These will be used to verify the particle tracking results and provide insight into the development time of the system.

Development of Particle Tracking Model

A particle tracking model will be used to simulate 3-dimensional transport in a circular pipe. Models will be constructed for both laminar and turbulent flow conditions with and without a reactive biofilm. The method of moments will be used to determine the effective one-dimensional transport parameters. For the case of no boundary reaction, the model results will be compared to the expressions developed by Taylor for the effective dispersion coefficient. For the case of a boundary reaction in laminar flow, the model results will be compared to the analytical expressions derived

for a first order boundary reaction. The development of the turbulent flow model will involve research into the nature of mass transport in the laminar sublayer of the flow field. Using a velocity profile developed by Wasan and Wilke (1963) and the universal velocity profile for the turbulent core, the nature of the effective dispersion coefficient is examined (without the effects of a biofilm) and compared to Taylor's result of $10.1au_*$. Finally, the model will be used to characterize the effective transport parameters for a turbulent flow system with a boundary reaction. No previous work was found on this topic so the model results cannot be verified with accepted results.

Analysis of Biofilm Characteristics and Diffusive Transport Parameters

The models discussed previously will be used to analyze the relationships between various biofilm characteristics and the effective transport parameters. Specifically the relationship between diffusion and reaction kinetics. A diffusion limited system is one in which the overall effective reaction term is dictated by the rate of transport into the biofilm. A non-diffusion or reaction rate limited system is one in which the effective reaction term is governed by the rate of decay within the biofilm. The nature of the effective transport parameters for both diffusion and reaction limited systems will be investigated. Also of interest is the nature of solute transport before the initial development time has elapsed. The effect of biofilm and pipe flow characteristics on the development time and the transport parameters at pre-development times will be investigated.

Chapter 2

Development of Particle Tracking Models

2.1 General Particle Tracking Theory: Random Walk Method

The particle tracking models used in this research are based on the Random Walk method of diffusion modeling. This is a statistical approach to describing the transport of solute at a molecular level. Molecular diffusion in a stagnant fluid is a constant process of random movements and collisions of particles. The extent of motion and collision is dependent on the nature of the fluid and the particles and can be characterized by the molecular diffusion coefficient. The Random Walk method aims to describe the random motion of single molecules and, through generalization, allows for the characterization of a large number of molecules in a system.

Suppose the motion of a single particle consists of random steps in one dimension to the left or right. The probability of the particle moving to the left is equal to probability of it moving to the right. In a given time interval, Δt, the particle may move a distance of Δx. On average, the motion of the particle will be such that it stumbles about the vicinity of the origin. However, after a given period of time, the particle will have moved sometimes to the left and sometimes right. The Central Limit Theorem shows that after m number of timesteps, the probability of the particle being located between $m\Delta x$ and $(m+1)\Delta x$ approaches the normal distribution with a mean of zero and a variance $\sigma^2 = t(\Delta x)^2 / \Delta t$ (Fischer, 1979). Therefore, it can be shown mathe-

matically that the probability of the particle being located at position *x* after an elapsed time *t* can be expressed as:

$$p(x, t) = \frac{1}{\sigma\sqrt{2\pi}} \exp\left(\frac{-x^2}{2\sigma^2}\right) \qquad \text{Eq. 2.1}$$

If the diffusion coefficient, *D*, is defined as $D = \Delta x^2/(2\Delta t)$, then the variance can be expressed as $\sigma^2 = 2Dt$ and Equation 2.1 can be rewritten as:

$$p(x, t) = \frac{1}{\sigma\sqrt{4\pi Dt}} \exp\left(\frac{-x^2}{4Dt}\right) \qquad \text{Eq. 2.2}$$

Now suppose that a group of particles, with initial locations at the origin, is confined to motion in one dimension. The motion of each individual particle is the same as that described above. After one time interval, approximately one half of the particles will have moved a distance Δx to the left and the other half a distance Δx to the right. After another timestep about one half of the group will have stepped back to the origin, one fourth would be located at $2\Delta x$, and one fourth at $-2\Delta x$. Given enough time, the group of particles would spread out with a higher density of particles at the origin and diminishing density as the distance from the origin increases. It is apparent that if the group of particles was located at the origin at time zero, the number of particles at any position *x* after time *t* would be proportional to the probability of any one particle being at position *x*. Therefore, Equation 2.2 can be expressed in terms of mass and concentration:

$$C(x, t) = \frac{M}{\sigma\sqrt{4\pi Dt}} \exp\left(\frac{-x^2}{4Dt}\right) \qquad \text{Eq. 2.3}$$

where *M* is the total mass of the particles normalized to the cross-sectional area. So the net outcome of the random walk method for a group of particles is a normal distribu-

tion of particles with a mean of zero and a standard deviation of $\sqrt{2Dt}$. It is important to note that the spreading of particles amounts to a net motion of particles from a higher concentration to a lower concentration. Furthermore, Equation 2.3 is the same result as that obtained by the solution of the one-dimensional diffusion equation.

2.2 Laminar Flow Models

The laminar flow models were constructed by extending the random walk method described previously to three dimensions, and then adding advection and a boundary reaction. Typically a two-dimensional, radial coordinate system is used to describe a circular pipe. This is possible due to the symmetry of the pipe's cross-section and it usually results in simpler transport equations. However, the theory behind the random walk method is more readily applied to a three-dimensional cartesian coordinate system than a radial coordinate system. While this leads to more complicated geometry, the complications involved with diffusion in the radial direction using the random walk approach are avoided.

Transport Within the Bulk Flow

Transport within the bulk flow is a result of two processes; advection and diffusion. Because the flow regime is laminar, transport in the lateral (cross-sectional) directions occurs as a result of molecular diffusion only. The reason being that, in laminar flow, streamlines are smooth and continuous. There are no turbulent eddies that may contribute to transport in any way. Advection is only in the longitudinal direction, therefore the only way a particle may move laterally is through molecular diffusion. Transport in the longitudinal (along the length of the pipe) direction occurs by both advection and diffusion. Incidentally, molecular diffusion in the longitudinal direction is practically negligible in comparison to advection. The following equation is used to describe the velocity profile for laminar flow conditions in a circular pipe:

$$u(r) = u_c - u_c\left(\frac{r}{a}\right)^2 \qquad \text{Eq. 2.4}$$

where u_c is the centerline (maximum) velocity of the pipe, a is the pipe radius and r is the radial location of the particle.

The run time of the model is broken up into a number of timesteps of length Δt. For each timestep, every particle is subject to random motion in each of the three dimensions according to the random walk theory. This random motion simulates transport due to molecular diffusion. At every timestep, and for every particle, a random number is generated for each of the three dimensions. In theory, the random numbers would have a standard normal distribution (mean of zero and standard deviation of one). Since the particle distribution was shown to have a mean of zero and a standard deviation of $\sqrt{2Dt}$ according to Equation 2.3, each random number is multiplied by the quantity $\sqrt{2D\Delta t}$, where D is the molecular diffusion coefficient.

Most random number generators produce uniform random numbers between -1 and 1. Therefore, an extra routine is required to convert them to standard normal variables. During an average simulation, the number of random numbers required is on the order of 10^{10}. The time spent converting each number to a standard normal variable is therefore quite considerable. The Central Limit Theorem, however, shows that if enough uniform random numbers are generated they will assume a normal distribution. The random number would then only have to be converted so that the standard deviation is one. This is achieved by multiplying each random number by $\sqrt{3}$, a fairly non-time consuming procedure. The end result, according to the Central Limit Theorem, is: if a large number of uniform random variables between $-\sqrt{3}$ and $\sqrt{3}$ are generated, they will assume a normal distribution with a mean of zero and a standard deviation of one. Each random variable would then have to be multiplied by $\sqrt{2D\Delta t}$ so that transport occurs in accordance with the random walk theory.

As mentioned previously, advection occurs only in the longitudinal direction.

The radial position of each particle at the beginning of the timestep is used to calculate the respective velocity according to Equation 2.4. The longitudinal location of the particle at the end of the timestep would be its beginning of timestep location, plus the product of the velocity and Δt, plus or minus any random motion due to diffusion (which would most likely be negligible). In summary, transport in the bulk flow can be expressed by the following set of equations:

$$y(t + \Delta t) = y(t) + \xi_1 \cdot \sqrt{2D\Delta t} \qquad \text{Eq. 2.5}$$

$$z(t + \Delta t) = z(t) + \xi_2 \cdot \sqrt{2D\Delta t} \qquad \text{Eq. 2.6}$$

$$x(t + \Delta t) = x(t) + u(r, t) \cdot \Delta t + \xi_3 \cdot \sqrt{2D\Delta t} \qquad \text{Eq. 2.7}$$

where y and z are the lateral directions, x is the longitudinal direction, and ξ_1, ξ_2, and ξ_3, are uniform random numbers between $-\sqrt{3}$ and $\sqrt{3}$. This set of equations is applied to each particle in the bulk flow at every timestep. If a particle encounters the pipe wall, it is reflected so that the angle of incidence equals the angle of reflection. The distance the particle travels from the reflection point is the same distance that it would have travelled beyond the pipe wall had it not been reflected.

Transport and Decay Within the Biofilm

Transport within the biofilm occurs by the process of molecular diffusion only. The models used in this research assume that there is no advection within the pore space of the biofilm. The application of the random walk method to transport within the biofilm is the same for that for the bulk flow. The only difference is that the bulk flow molecular diffusion coefficient, D, is different than the biofilm molecular diffusion coefficient D_b. The relationship between D and D_b is not exactly understood and

has been the subject of considerable research in the past. Zhang and Bishop in 1994 performed an intensive study that showed the relationships between the ratio D_b/D, biofilm porosity and tortuosity. Porosity is defined as the ratio of the pore volume to the total biofilm volume and tortuosity is defined as the ratio of the effective (actual) pore/capillary length to the biofilm thickness. The results of the study show that a general definition for the biofilm diffusion coefficient, D_b, is:

$$D_b = \frac{n}{\tau^2} D \qquad \text{Eq. 2.8}$$

where n is the porosity and τ is the tortuosity. The following equations describe transport within the biofilm region:

$$y(t + \Delta t) = y(t) + \xi_1 \cdot \sqrt{2 D_b \Delta t} \qquad \text{Eq. 2.9}$$

$$z(t + \Delta t) = z(t) + \xi_2 \cdot \sqrt{2 D_b \Delta t} \qquad \text{Eq. 2.10}$$

$$x(t + \Delta t) = x(t) + \xi_3 \cdot \sqrt{2 D_b \Delta t} \qquad \text{Eq. 2.11}$$

This set of equations is applied to each particle in the biofilm at every timestep.

In order to simulate the effects of a boundary reaction, any particle located within the biofilm loses mass by either a first order or zero order reaction. The mass of each particle decays according to the following equation for a zero order reaction:

$$Mass(t + \Delta t) = Mass(t) - k_0 \Delta t_{bio} \qquad \text{Eq. 2.12}$$

where k_0 is the zero order reaction rate and Δt_{bio} is the length of time the particle is in the biofilm. The particle may remain in the biofilm for the entire timestep, may leave

the biofilm at some time during the timestep, or may enter the biofilm at some point during the timestep. If the reaction is first order, the following backward difference equation is used to compute the decay of each particle in the biofilm (because the timestep length is so short a linear approach to a non linear equation is acceptable):

$$Mass(t + \Delta t) = Mass(t) - k_1 Mass(t)\Delta t_{bio} \qquad \text{Eq. 2.13}$$

where k_1 is the first order decay constant (a positive decay constant represents a decay).

Bulk Flow - Biofilm Interface Condition

At any point within a given timestep, a particle may come in contact with the bulk flow - biofilm interface. When this occurs, it has to be decided whether the particle will enter the biofilm or reflect off it and remain in the bulk flow. At the interface there is no advection because the velocity of a fluid at a solid boundary must be zero (in compliance with the no-slip condition). Therefore, molecular diffusion is the only factor controlling the motion of the particle at the boundary. Since the molecular diffusion coefficient is usually different for the two regions, the probability of the particle diffusing to one side of the interface will be different than the probability of diffusion to the other side. A probability rule was developed to make this determination.

Suppose a slug of tracer is injected at the boundary between two regions with different molecular diffusion coefficients. After a given amount of time, the concentration profile will approach a distribution that is skewed to the side with the greater diffusion coefficient. The percentage of the total mass residing in one of the two regions represents the probability of any particular particle diffusing to that region. In other words, if an equal percentage of mass is located in the two regions after a given amount of time, then a particle located at the interface has the same probability of dif-

fusing to one side of the interface as the other side. If 75% of the mass is located to the left of the interface, then a particle located at the interface has a 75% chance of diffusing to left and a 25% chance of diffusion to the right. This probability must be expressed in terms of the biofilm and bulk flow characteristics if it is to be used for modeling purposed. This is accomplished through the solution of the diffusion equation in an infinite 2-region medium with the interface at x=0. Since the timestep used in the particle tacking model is very small, the new position of a particle originating at the interface will be close to the interface itself. The influence of other boundaries is not felt during a small timestep. Thus, it is reasonable to develop a probability rule for determining the particle position assuming an infinite medium on either side of the interface.

The one-dimensional diffusion equation for a two region system with the interface at the origin (x = 0) is written as:

$$\frac{\partial C}{\partial t} = nD_1\frac{\partial^2 C}{\partial x^2}, \text{ Region 1 - } x > 0$$

$$\frac{\partial C}{\partial t} = nD_2\frac{\partial^2 C}{\partial x^2}, \text{ Region 2 - } x < 0 \qquad \text{Eq. 2.14}$$

The two boundary conditions for this set of equations are: equal concentrations at the interface and equal flux at the interface. If region 1 is the bulk flow and region 2 is the biofilm, then n is equal to 1.0 when x > 0 and D_1 and D_2 can be referred to as D and D_b, respectively. Solving Equation 2.14 using the new notation for the percent mass in the bulk flow, results in the following expression for p (the probability that a particle located at the bulk flow - biofilm interface will diffuse into the bulk):

$$p = \frac{1}{1 + n\sqrt{D_b / D}} \qquad \text{Eq. 2.15}$$

where n is the porosity of the biofilm. For use in the model, p must be rescaled so that a probability of zero is represented by -1 and a probability of one is represented by 1

because the random number generator generates random numbers with a uniform distribution between -1 and 1. The rescaled probability will be denoted, p_n.

During a model simulation, if a particle reaches the interface (whether coming from the biofilm or the bulk flow), a random number between -1 and 1 is generated. If the random number is greater than p_n, the particle will diffuse into the biofilm. If the random number is less than p_n, the particle will diffuse into the bulk flow. Therefore, if the probability of a particle diffusing to the bulk flow is 1.0, then no particle will enter the biofilm because a random number greater than 1.0 will never be generated. If the probability of a particle diffusing to the bulk flow is 0.5 (represented as 0.0 when rescaled to p_n), then the particle has an equal chance of entering the biofilm as the bulk flow (because half the time the random number will be greater than 0.0 and half the time less than 0.0). As shown in Equation 2.15, the probability rule is a function of porosity and the ratio D/D_b. To give an example of the effects of porosity on the particle behavior at the interface, assume that the biofilm porosity is zero. If this is the case, a particle should never enter the biofilm because there is no available pore space in which to go. Equation 2.15 computes a probability of 1, so the particle will never enter the biofilm. Now assume that the porosity of the biofilm is 1 (this is the same porosity as the bulk flow) and the diffusion coefficients for both regions are equal (D/D_b =1). We would expect that a particle located at the interface would diffuse to either region with equal probability because the characteristics of both regions are the same. For this case the probability, p, is 0.5 (rescaled to p_n = 0.0), so the particle will behave as expected. This probability rule ensures that particles will behave accordingly at the interface.

Timestep Restrictions

The random walk method of particle tracking is only accurate when certain restrictions are placed on the timestep (Δt) and the size of the typical displacement by

diffusion (Δx) during Δt. Both Δt and Δx must be several orders of magnitude smaller than the total time and space scale of the simulation. The time and space intervals must also be much smaller than those of any physical phenomenon occurring within the system. For example, the time and space intervals would have to be much smaller than those of any turbulent eddies that may exist in the system in order to fully capture their effects on transport.

Since, the distance travelled by any particle in a given timestep is directly related to the timestep length, it is only necessary to restrict the timestep length used in simulation. As stated above, the time interval, Δt, must be much smaller than the observation time and must be small enough so that the diffusion step is much smaller than observation space. Therefore, the timestep should be limited so that the largest diffusion step (space interval) is smaller than 1% of the pipe radius. The largest possible diffusion step is $\sqrt{3}\sqrt{2D\Delta t}$ where $\sqrt{3}$ is the largest random number generated. This restriction takes the following form:

$$\Delta t < \frac{(0.01a)^2}{6D} \qquad \text{Eq. 2.16}$$

Also, a particle should not be able to diffuse through the entire depth of the biofilm in any timestep. To be conservative, this restriction limits the space interval to half the biofilm thickness and takes the following form:

$$\Delta t < \frac{(0.5b_t)^2}{6D_b} \qquad \text{Eq. 2.17}$$

where b_t is the biofilm thickness. Finally, the timestep must be much smaller than the timescale associated with decay in the biofilm. Therefore $\Delta t << 1/k_1$ where k_1 is the first order decay constant.

2.3 Turbulent Flow Models

The extension of the random walk method to turbulent flow in a pipe is slightly more complicated. Transport and reaction within the biofilm remains the same and the interface condition still holds true, but some changes are required in the description of the bulk flow mass transport. Since rotational eddies exist in a turbulent flow field, transport in the lateral directions is no longer only a result of molecular diffusion. A cross-sectional mixing coefficient, termed the eddy diffusivity, has to be developed to replace the diffusion coefficient in the transport equations. Unlike the diffusion coefficient, the eddy diffusivity is a function of the particle's radial location. Also, a different velocity profile will have to be developed that applies to turbulent flow within a circular pipe. The universal velocity profile, otherwise known as the logarithmic velocity profile (discussed in Chapter 1), accurately describes the velocity field in the turbulent core. Finally, boundary layer theory and experimentation show that a laminar sublayer exists between the pipe wall and the turbulent core. In the laminar subregion, which is usually extremely thin, transport occurs as a result of molecular diffusion. Therefore, the diffusivity will have to be adjusted for this region. Furthermore, a different velocity profile is required for the laminar sublayer. A description of the background theory to turbulent flow as it applies to Taylor dispersion can be found in Chapter 1.

Mass Transport in the Vicinity of the Pipe Wall

Typically when describing fully turbulent flow within a pipe, the flow regime is divided into three distinct zones; the laminar sublayer, a buffer zone, and the turbulent core. In the turbulent core, which encompasses the vast majority of the flow regime, inertial forces dominate and viscous forces can be neglected. This is the standard definition of turbulent flow. As discussed previously, laminar boundary layer theory dictates that near a solid boundary the viscous forces must become significant at least

within some small region near the boundary. In turbulent flow, the region where viscous forces cannot be neglected consists of both the laminar sublayer and the buffer zone. In the laminar sublayer, viscous forces dominate and inertial forces can be neglected. In the buffer zone, both viscous and inertial forces must be retained. The logarithmic law can be used to specify the velocity profile in each of the zones thus resulting in a continuous velocity profile across the pipe cross section.

While the analysis just described is useful for determining turbulent flow velocities, it is not valid for describing turbulent transport in the vicinity of the pipe wall. The concept of three different fluid layers leads to an unrealistic discontinuity in the eddy diffusivity function. While the three separate functions to describe the velocities in each layer are continuous, their first derivatives, which are used to calculate the eddy diffusivity, are not continuous. Furthermore, the Reynold's analogy, which is used to derive expressions for the eddy diffusivity, breaks down near the wall. The Reynold's analogy for turbulent flow assumes that transport of mass is equal to transport of momentum. This relationship is expressed by the Schmidt number, defined as follows for the laminar region:

$$Sc = \frac{\text{momentum transport}}{\text{mass transport}} = \frac{\upsilon}{D} \qquad \text{Eq. 2.18}$$

where D is the molecular diffusion coefficient and υ is the kinematic viscosity. For the Reynold's analogy to be valid, the Schmidt number has to equal one, which obviously would not be the case in the laminar sublayer. Therefore, in order to effectively describe mass transfer near the pipe wall, the Reynold's analogy must be abandoned near the wall region (it still is valid in the turbulent core) and expressions for the velocity and eddy diffusivity that are continuous with the turbulent core must be developed.

In 1963, Wasan, Tien, and Wilke pointed out that most of the proposed eddy viscosity distributions do not satisfy the theoretical criterion which stated that the tur-

bulent contribution to the Reynold's stress $\overline{u}_i\overline{v}_i$ near the wall is proportional to y^n, where n is not less than three (Wasan and Tien, 1963) (u_i is the fluctuating velocity in the axial direction, v_i is the fluctuating velocity in the radial direction and y is the distance from the pipe wall). They also showed that from velocity variation data and turbulent shear stress data, the degree of turbulence in the moving fluid varies continuously from the wall to the pipe axis. Therefore, the concept of three distinct layers would be incorrect (Wasan and Wilke, 1964). By using the equations of mean motion and the universal velocity profile for the turbulent core, Wasan, Tien, and Wilke developed theoretical expressions for the continuous variation of velocity and eddy diffusivity for the wall region of pipe flow.

Since the wall region is very thin, a Taylor series expansion was used to describe the velocities. Likewise, the time averaged turbulent shear stress was also expressed as a Taylor series. Using boundary conditions and neglecting the insignificant terms, the dimensionless forms of the velocity and turbulent shear stress are given as:

$$u^+ = y^+ + U_4{}^+(y^+)^4 + U_5{}^+(y^+)^5 \qquad \text{Eq. 2.19}$$

$$\overline{u_i v_i}^+ = -4U_4{}^+(y^+)^3 - 5U_5{}^+(y^+)^4 \qquad \text{Eq. 2.20}$$

where u^+ is the dimensionless, time averaged velocity at any point (u/u_*, where u_* is the shear velocity), $\overline{u}_i\overline{v}_i{}^+$ is the dimensionless turbulent shear stress ($\overline{u}_i\overline{v}_i/u_*{}^2$), and y^+ is the dimensionless distance from the pipe wall (yu_*/υ). In the wall region the shear stress can be considered constant and the flow is determined by the wall shear stress, the fluid viscosity and the distance from the wall. Therefore, the coefficients $U_4{}^+$ and $U_5{}^+$ are universal constants (Wasan and Tien, 1963). In order to calculate $U_4{}^+$ and $U_5{}^+$, the values of u^+ and its first and second derivatives are matched with the univer-

sal velocity profile in the turbulent core. This results in a smooth transition at y^+ equal to 19.7138. Using the calculated values for the coefficients, Equation 2.19 can be rewritten to describe the velocity distribution for $y^+ < 19.7138$:

$$u^+ = y^+ - 1.09833 \cdot 10^{-4}(y^+)^4 + 3.30083 \cdot 10^{-6}(y^+)^5 \qquad \text{Eq. 2.21}$$

Likewise, Equation 2.20 can be rewritten to describe the time averaged turbulent shear stress for $y^+ < 19.7138$:

$$\overline{u_i v_i}^+ = 4.39332 \cdot 10^{-4}(y^+)^3 - 16.5041 \cdot 10^{-6}(y^+)^4 \qquad \text{Eq. 2.22}$$

Using Equation 2.21 and Equation 2.22, the following expression for the ratio of eddy diffusivity (or eddy viscosity) to kinematic viscosity is given as:

$$\frac{\varepsilon}{\upsilon} = \frac{\overline{u_i v_i}^+}{du^+/dy^+} = \frac{4.39332 \cdot 10^{-4}(y^+)^3 - 16.5041 \cdot 10^{-6}(y^+)^4}{1 - 4.39332 \cdot 10^{-4}(y^+)^3 + 16.5041 \cdot 10^{-6}(y^+)^4} \qquad \text{Eq. 2.23}$$

Equation 2.23 gives the distribution of the eddy diffusivity for the wall region ($y^+ <$ 19.7138). It results in a smooth transition to the eddy diffusivity in the turbulent core. Expressions for the velocity and eddy diffusivity in the turbulent core are developed in the following section.

Mass Transport in the Turbulent Core

As discussed previously, the universal velocity profile accurately describes the velocity in the turbulent core. From Equation 1.15, the velocity is expressed as:

$$u^+ = 5.5 + 2.5 \ln y^+ \qquad \text{Eq. 2.24}$$

From the Reynold's analogy, the eddy diffusivity in the turbulent core is defined as (from Equation 1.16):

$$\varepsilon = -\frac{m}{\partial C/\partial r} = -\frac{\tau}{\rho\frac{\partial u}{\partial r}} - \upsilon = -\frac{\tau_w(r/a)}{\rho\frac{\partial u}{\partial r}} - \upsilon \qquad \text{Eq. 2.25}$$

where ε is the eddy diffusivity, m is the rate of radial transfer of matter of concentration C, τ is the shear stress, τ_w is the wall shear stress, r is the radial coordinate, a is the pipe radius, and ρ is the fluid density.

To be consistent with Equation 2.24 and the expressions for velocity and diffusivity in the wall region, the diffusivity in the turbulent core should be expressed in terms of y^+. Using Equation 2.24, Equation 2.25 and the following definitions: $\tau_w = u_*^2\rho$ and $y^+ = (a-r)u_*/\upsilon$, the ratio of eddy diffusivity to kinematic viscosity can be expressed as:

$$\frac{\varepsilon}{\upsilon} = 0.4y^+\left(1 - \frac{y^+\upsilon}{au_*}\right) - 1 \qquad \text{Eq. 2.26}$$

Equation 2.26 gives the eddy diffusivity distribution from $y^+ > 19.7138$ to the center of the pipe.

Velocity and Diffusivity Profiles

Figure 2.1 shows the velocity distribution from the wall to the pipe axis using Equation 2.21 and Equation 2.24.

Figure 2.1: Dimensionless Velocity Distribution (Wall to Pipe Axis)

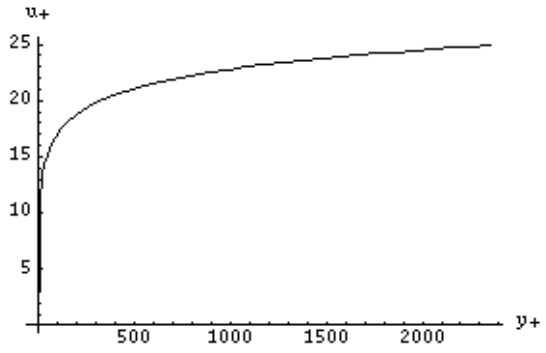

Figure 2.2 shows the velocity distribution in the vicinity of the pipe wall. Notice that the transition from the wall region to the turbulent core is smooth and continuous.

Figure 2.2: Dimensionless Velocity Distribution (Wall Region - Turbulent Core)

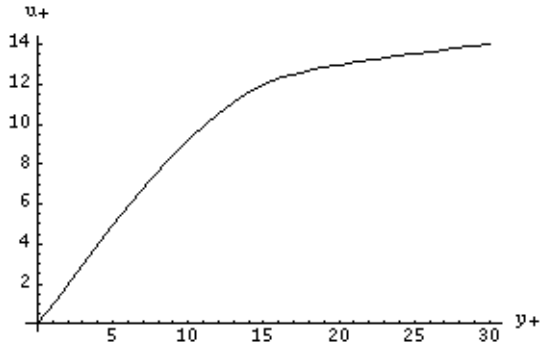

Equation 2.23 and Equation 2.26 are used to define the ratio of eddy diffusivity to kinematic viscosity for the entire pipe region. Figure 2.3 shows this distribution from the pipe wall to the pipe axis. Notice that the diffusivity approaches zero (it actually approaches the molecular diffusion coefficient) at both the wall and the center of the pipe. Near the wall the slope of the velocity curve is very large thus producing a small diffusivity. Near the center of the pipe the shear stress approaches zero. The result is that transport at the wall and the center of the pipe occurs by molecular diffusion. The greatest diffusivity values occur halfway between the pipe wall and the pipe axis where the most turbulence exists.

Figure 2.3: Diffusivity/Viscosity Distribution (Wall to Pipe Axis)

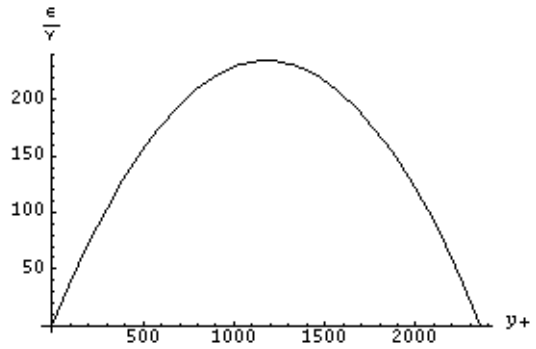

Equation 2.23 predicts that the diffusivity will go to zero at the pipe wall. This is not entirely accurate. At the pipe wall, laminar flow conditions exist and transport will occur by molecular diffusion. Therefore when solving for diffusivity, the molecular diffusion coefficient, *D*, must be added to both Equation 2.23 and Equation 2.26. Once this modification has been made, the diffusivity approaches *D* as expected (see Figure 2.4 where $D = 1x10^{-5}$ cm^2/s).

Figure 2.4: Eddy Diffusivity in Wall Region

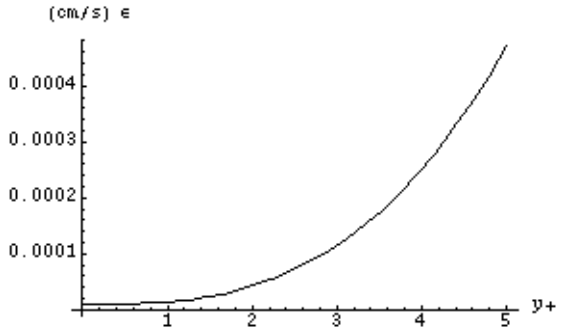

Figure 2.5 shows the distribution of the eddy diffusivity - kinematic viscosity ratio for the wall region and part of the turbulent core. Notice that the profiles are continuous across the boundary between the two regions.

Figure 2.5: Diffusivity/Viscosity Distribution (Wall Region - Turbulent Core)

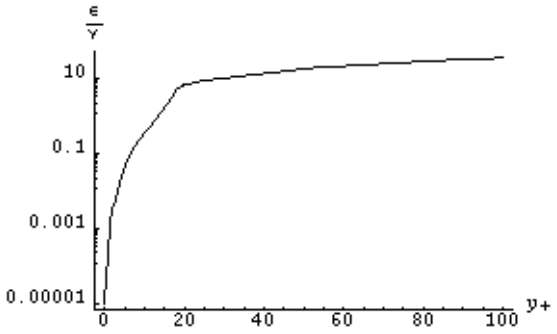

Bulk Flow Transport Step Equations

Since transport in the biofilm and the interface conditions are identical for both laminar and turbulent flow, only the bulk flow transport equations need to be modified for the turbulent flow model. As with the laminar flow model, advection only occurs in the longitudinal direction and is a function of the particles' velocity at a given location. The random step is the same as in the laminar model except the diffusion coefficient is replaced by the eddy diffusivity, which is now radially dependent.

In particle tracking models, when the dispersive term is spatially dependent, as it is in turbulent flow, an additional term must be added to the step equation (Tompson, 1988). It is based on the gradient of the diffusivity and acts as a correction term to keep particles away from areas of low velocity. The bulk flow transport step equations can now be written as:

$$y(t+\Delta t) = y(t) + \xi_1 \cdot \sqrt{2\varepsilon(y^+, t)\Delta t} + \frac{\partial}{\partial y}(\varepsilon(y^+, t))\Delta t \qquad \text{Eq. 2.27}$$

$$z(t+\Delta t) = z(t) + \xi_2 \cdot \sqrt{2\varepsilon(y^+, t)\Delta t} + \frac{\partial}{\partial z}(\varepsilon(y^+, t))\Delta t \qquad \text{Eq. 2.28}$$

$$x(t+\Delta t) = x(t) + u(y^+, t)\Delta t + \xi_3 \cdot \sqrt{2\varepsilon(y^+, t)\Delta t} \qquad \text{Eq. 2.29}$$

For the step term in the axial direction, the value for the lateral diffusivity is used. It is assumed that the lateral diffusivity is equal to the longitudinal diffusivity. Also, the diffusivity gradient correction term is not necessary in the axial direction.

Timestep Restrictions

For turbulent flow, the time-space restrictions are similar to those of the laminar flow model. However, since turbulent flow contains eddies, and transport in the lateral direction is a result of these eddies and internal turbulence, the timestep much be much smaller than for laminar flow in order to capture this physical phenomenon.

As in laminar flow, the timestep must be much smaller that $1/k_1$ in order to represent exponential decay with a linear approximation. Also, a particle should not be able to travel across the entire biofilm in a single timestep. Therefore, to be conservative:

$$\Delta t < \frac{(0.5 b_t)^2}{6 D_b} \qquad \text{Eq. 2.30}$$

Finally, a particle should not be able to travel laterally more than a distance of 1% of the radius in a single timestep. Lateral transport is a result of the eddy diffusivity and the diffusivity gradient correction term. Therefore, Δt must be chosen such that

$$0.01a > \sqrt{3}\sqrt{2\varepsilon_{max}\Delta t} + \left(\frac{\partial \varepsilon}{\partial y}\right)_{max}\Delta t \qquad \text{Eq. 2.31}$$

where $\sqrt{3}$ is the maximum value of the random term, ε_{max} is the maximum possible value for the eddy diffusivity and $(\partial\varepsilon/\partial y)_{max}$ is the maximum possible value for the diffusivity gradient correction term. The timestep dictated by Equation 2.31 is almost invariably the controlling factor in choosing the proper timestep length. Since the wall region of the flow field is very thin, it is important that the timestep is small enough to

capture the detail of the velocity and diffusivity profiles in this region. However, the dispersion coefficient in the wall region is very small (approaches the molecular diffusion coefficient) so the timestep specified by Equation 2.31 is more than adequate to ensure proper behavior in the wall region.

2.4 System Characterization

Various physical parameters are required to describe both the bulk flow and the biofilm regions. The main parameters required to describe the bulk flow are the radius of the pipe, the Reynold's number, the molecular diffusion coefficient and the velocity profile. The velocity profiles are dependant upon whether the flow is laminar or turbulent and are described in detail previously. The radius of the pipe is basically chosen as a matter of convenience depending upon a particular simulation. For the laminar flow simulations, the pipe radius was chosen to be 0.8 cm unless otherwise specified. This is the same value used for Tim Cox's research and in the Horn and Hempel experiments. The range of molecular diffusion coefficients given in literature is 10^{-4} to 10^{-6} cm/s (Chapra, 1997). Unless otherwise stated, the molecular diffusion coefficient was chosen to be the average value of 10^{-5} cm/s. The Reynold's number was varied over several orders of magnitude for different simulations to show the dependence (or lack thereof) of the transport parameters on Reynold's number.

The physical parameters required to describe the biofilm coating are its thickness, porosity, diffusion coefficient, and decay constant. Values given in literature for typical biofilm thicknesses are in the range of 0.004 - 0.05 cm (Cox, 1997). For most of the simulations, a biofilm thickness of 0.035 cm is used. This is the value used in the Horn and Hempel experiments as well as Tim Cox's research. However, a sensitivity analysis is performed to show the effects of biofilm thickness on the bulk transport parameters. Biofilm porosities are given in the range of 0.58 - 0.93 with an average of 0.7 - 0.75 (Zhang and Bishop 1, 1994). Unless otherwise stated, a porosity of 0.73 is used in the simulations. Molecular diffusion in biofilms is usually described with a

ratio of the biofilm diffusion to bulk flow diffusion. This ratio is shown to be dependant upon the biofilm porosity and tortuosity (Zhang and Bishop 2, 1994). Considering the range of values given for porosity and tortuosity in biofilms, Equation 2.8 can be used to calculate the possible values for the ratio of biofilm diffusion to bulk flow diffusion. The calculated range is 0.36-0.81 with an average of 0.55-0.6. In the simulations, the biofilm diffusion coefficient is chosen to be 60% of the bulk flow diffusion. A sensitivity analysis is performed to show the model sensitivity to both porosity and biofilm diffusion.

The rate constants used to describe the reactions occurring in the biofilm are dependent upon both the makeup of the biofilm and the reactive constituent. Since there is no particular type of solute or biofilm being studied in this research, there is no specific range of values for the decay constant. In general, first order rate constants are on the order of -1.0/s (Cox, 1997). The value used in simulation varies and will be specified with the simulation results.

Chapter 3

Analytical Solution to Transport in Laminar and Turbulent Flow

3.1 Laminar Flow Solutions

Aris' Method of Moments can be applied to the advection-diffusion equation to analytically determine the one-dimensional effective parameters. The following analysis assumes that the flow field in the pipe is laminar, and that the boundary reaction is a first order process. The zeroth, first and second concentration moments can be used, as described previously, to determine the effective decay coefficient, the effective velocity, and the effective longitudinal dispersion.

Equation 1.2, when rewritten with a reaction term, takes the following form:

$$n\frac{\partial C}{\partial t} + nu(r)\frac{\partial C}{\partial x} - \frac{1}{r}\frac{\partial}{\partial r}\left(nD_r\frac{\partial C}{\partial r}\right) - \frac{\partial}{\partial x}\left(nD_x\frac{\partial C}{\partial x}\right) - nkC = 0 \qquad \text{Eq. 3.1}$$

where k is the first order decay constant. In this equation, a positive value for k represents a decay. In order to compute the p^{th} concentration moment, Equation 3.1 must be multiplied by $x^p dx$ and then integrated from $x = +\infty$ to $x = -\infty$. The resulting equation is:

$$\int_{-\infty}^{+\infty} x^p n\frac{\partial C}{\partial t} r dx + \int_{-\infty}^{+\infty} x^p nru(r)\frac{\partial C}{\partial x} dx - \int_{-\infty}^{+\infty} x^p \frac{\partial}{\partial r}\left(nrD_r\frac{\partial C}{\partial r}\right) dx \qquad \text{Eq. 3.2}$$
$$- \int_{-\infty}^{+\infty} x^p n\frac{\partial}{\partial x}\left(rD_x\frac{\partial C}{\partial x}\right) dx - \int_{-\infty}^{+\infty} x^p kC dx = 0$$

Using integration by parts on each of the terms in Equation 3.2, and applying the boundary condition that at $x = \infty$, the concentration is zero, the following equation is derived in terms of C_p:

$$n\frac{\partial C_p}{\partial t} - upnC_{p-1} - \frac{1}{r}\frac{\partial}{\partial r}\left(nrD\frac{\partial C_p}{\partial r}\right) - Dpn(p-1)C_{p-2} - nkC_p = 0 \qquad \text{Eq. 3.3}$$

If longitudinal diffusion is considered negligible, the fourth term in Equation 3.3 can be set to zero.

Solution for the Effective Decay Constant

In order to develop an expression for the effective decay constant, the zeroth concentration moment must first be determined. Equation 3.3, when written in terms of C_0, takes the following form:

$$n\frac{\partial C_{0i}}{\partial t} - \frac{1}{r}\frac{\partial}{\partial r}\left(nrD_i\frac{\partial C_{0i}}{\partial r}\right) - nkC_{0i} = 0,\text{""}i = 1, 2 \qquad \text{Eq. 3.4}$$

Equation 3.4 applies to the bulk flow and biofilm regions of the pipe ($i = 1$ for bulk flow and $i = 2$ for the biofilm region), where $k = 0$ and $n = 1$ in the bulk flow region. Three boundary conditions are required to solve the two equations; a no flux condition at the pipe wall, equal concentrations at the bulk flow / biofilm interface and equal flux at the interface. These boundary conditions are written, respectively, as:

$$nD_2\frac{\partial C_{02}}{\partial r} = 0, at\ r = b \qquad \text{Eq. 3.5}$$

where b is the radial distance to the pipe wall,

$$C_{01} = C_{02}, \text{at } r = a \qquad \text{Eq. 3.6}$$

where a is the distance to the bulk flow / biofilm interface, and

$$-D_1 \frac{\partial C_{01}}{\partial r} = -nD_2 \frac{\partial C_{02}}{\partial r}, \text{at } r = a \qquad \text{Eq. 3.7}$$

Using the discontinuous weighing function theory from boundary value problems in heat conduction (which is analogous to mass transport in a fluid) the solution to Equation 3.4 can be written:

$$C_{0i}(r, t) = \sum_{n=1}^{\infty} A_n X_{in}(r) \Gamma_{in}(t) \Rightarrow i = 1, 2 \qquad \text{Eq. 3.8}$$

where n is the eigenvalue index, $X_{in}(r)$ are the radial eigenfunctions, $\Gamma_{in}(t)$ describes the temporal behavior associated with the n^{th} eigenvalue, and A_n is a constant coefficient (Cox, 1997). Combining Equation 3.8 and Equation 3.4, the following expressions are obtained:

$$\begin{aligned} \Gamma_{1n}(t) &= \exp(\lambda_{1n}^2 t) \\ \Gamma_{2n}(t) &= \exp((\lambda_{2n}^2 - k)t) \end{aligned} \qquad \text{Eq. 3.9}$$

$$\begin{aligned} X_{1n}(r) &= J_0(\beta_{1n} r) \\ X_{2n}(r) &= C_{2n} I_0(\beta_{2n} r) + B_{2n} K_0(\beta_{2n} r) \end{aligned} \qquad \text{Eq. 3.10}$$

where λ_{in} is the n^{th} eigenvalue for either region 1 (bulk flow) or region 2 (biofilm). The eigenvalues for the two regions are related as follows:

$$\lambda_{1n}^2 = \lambda_{2n}^2 - k \qquad \text{Eq. 3.11}$$

where λ_{1n}^2 must be less than zero and therefore λ_{2n}^2 must be less than k. In Equation 3.10, J_0 is the zero order Bessel Function of the first and second kind and I_0 and K_0 are the zero order, Modified Bessel Functions of the first and second kind, respectively. β_{1n} and β_{2n}, used for simplicity, are defined as:

$$\beta_{1n} = \sqrt{-\lambda_{1n}^2 / D_1}$$
$$\beta_{2n} = \sqrt{\lambda_{2n}^2 / D_2} \qquad \text{Eq. 3.12}$$

C_{2n} and B_{2n} are constants that can be solved for by using the boundary conditions defined by Equation 3.5 and Equation 3.6. The resulting expressions are given below and can be solved simultaneously through substitution:

$$C_{2n} = \frac{B_{2n} K_1(\beta_{2n} b)}{I_1(\beta_{2n} b)} \qquad \text{Eq. 3.13}$$

$$B_{2n} = \frac{J_0(\beta_{1n} a) - C_{2n} I_0(\beta_{2n} a)}{K_0(\beta_{2n} a)} \qquad \text{Eq. 3.14}$$

where I_1 and K_1 are first order Modified Bessel Functions of the first and second kind, respectively.

The eigenvalues for the system can be determined by applying the equal flux boundary condition, defined by Equation 3.7, to the expressions for C_{01} and C_{02} (Equation 3.4). The resulting transcendental equation is written as:

$$D_1 \beta_{1n} J_1(\beta_{1n} a) = -n_2 D_2 \beta_{2n} (C_{2n} I_1(\beta_{2n} a) - B_{2n} K_1(\beta_{2n} a)) \qquad \text{Eq. 3.15}$$

where β_{1n} and β_{2n} are related by Equation 3.11. The roots of the transcendental equation are the eigenvalues for the system.

The remaining unknown coefficient from Equation 3.8, A_n, is solved for using the Orthogonal-Expansion Technique from heat transport. The reader is referred to

Cox, 1997 for the details of this solution, which will not be discussed here. The solution for A_n is of the following form:

$$A_n = \frac{\int_0^a f_1 J_0(\beta_{1n} r) r dr + n_2 \int_a^b f_2 (C_{2n} I_0(\beta_{2n} r) + B_{2n} K_0(\beta_{2n} r)) r dr}{\int_0^a J_0^2(\beta_{1n} r)^2 r dr + n_2 \int_a^b (C_{2n} I_0(\beta_{2n} r) + B_{2n} K_0(\beta_{2n} r))^2 r dr} \qquad \text{Eq. 3.16}$$

where f_1 and f_2 are the initial conditions for C_0 for the bulk flow and the biofilm region, respectively.

The above expressions can be used to reach a solution for C_0. A computer code is used to determine the eigenvalues that solve the equations. Since C_0 gives the concentration moment at a single position *r*, it must be integrated over the pipe cross section to determine the mass moment, M_0:

$$M_0 = \sum_{n=1}^{\infty} 2\pi A_n \exp(\lambda_{1n}^2) \cdot \frac{a}{\beta_{1n}} J_1(\beta_{1n} a) \qquad \text{Eq. 3.17}$$

Then using Equation 1.21 the following expression can be derived for the effective one-dimensional decay constant:

$$k^*(t) = \frac{dM_0/dt}{M_0} = \frac{\sum_{n=1}^{\infty} 2\pi A_n \exp(\lambda_{1n}^2) \cdot \frac{a}{\beta_{1n}} J_1(\beta_{1n} a) \lambda_{1n}^2}{\sum_{n=1}^{\infty} 2\pi A_n \exp(\lambda_{1n}^2) \cdot \frac{a}{\beta_{1n}} J_1(\beta_{1n} a)} \qquad \text{Eq. 3.18}$$

After a large enough development time, the effective decay coefficient reaches an asymptotic value. When this occurs, it can be seen that k^* converges on ${\lambda_1}^2$ where λ_1 is the region 1 eigenvalue closest to 0.0.

Solution for Effective Velocity

To solve for the first moment of concentration, Equation 3.3 takes the form:

$$n\frac{\partial C_{1i}}{\partial t} - unC_{0i} - \frac{1}{r}\frac{\partial}{\partial r}\left(nrD_i\frac{\partial C_{1i}}{\partial r}\right) - nkC_{1i} = 0 \Rightarrow i = 1, 2 \qquad \text{Eq. 3.19}$$

The same boundary conditions apply as described by Equation 3.5, Equation 3.6, and Equation 3.7. The solution, again from heat conduction theory, is written as:

$$C_{1i}(r, t) = \sum_{n=1}^{\infty} X_{in}(r)\Gamma_{in}(t) \Rightarrow i = 1, 2 \qquad \text{Eq. 3.20}$$

Because the same boundary conditions exist for this problem, the spatial solution is the same as that derived for C_0. Plus, the application of the boundary condition described by Equation 3.7 (equal flux at the interface between regions), assures that the eigenvalues will be the same (Cox, 1997). Therefore, the spatial solution is written as:

$$X_1(r) = J_0\left(\sqrt{\frac{-\lambda_1^2}{D_1}}r\right) \qquad \text{Eq. 3.21}$$

where λ_1 is the eigenvalue closest to 0.0.

The temporal solution to the problem is written as:

$$\Gamma_1(t) = \exp(\lambda_1^2 t)Lt \qquad \text{Eq. 3.22}$$

where L is expressed as:

$$L = \frac{A_n \int_0^a u_1(r) J_0^2(\beta_1 r) r dr}{\int_0^a J_0^2(\beta_1 r) r dr} \qquad \text{Eq. 3.23}$$

Integrating the equation for C_1 over the cross sectional area of the pipe, the following expression is obtained for the first moment of mass:

$$M_1 = 2\pi \exp(\lambda_1^2 t) Lt\left(\frac{a}{\beta_1} J_1(\beta_1 a)\right) \qquad \text{Eq. 3.24}$$

From Equation 1.23 and Equation 3.17 the position of the centroid is:

$$\overline{X} = \frac{Lt}{A_n} \qquad \text{Eq. 3.25}$$

and applying Equation 1.24, the effective velocity is:

$$U_{eff} = \frac{d\overline{X}}{dt} = \frac{L}{A_n} \qquad \text{Eq. 3.26}$$

Solution for the Effective Dispersion Coefficient

Equation 3.3, when used to solve for the second concentration moment, can be written as:

$$n\frac{\partial C_{2i}}{\partial t} - 2unC_{1i} - \frac{1}{r}\frac{\partial}{\partial r}\left(nrD_i \frac{\partial C_{2i}}{\partial r}\right) - 2D_i nC_{0i} - nkC_{2i} = 0 \qquad \text{Eq. 3.27}$$

To develop expressions for the effective dispersion coefficient is it necessary to use the full expressions for C_0, C_1 and C_2. Applying integral transforms to these equations results in a system of analytical expressions that can be used to determine D^*. The

eigenvalues are the same as those used in the C_0 solution.

3.2 Turbulent Flow Solution

A set of analytical solutions for the effective, one-dimensional transport parameters in a turbulent flow setting with a boundary reaction is too complicated to derive. Therefore, the turbulent flow model with the reactive biofilm cannot be verified analytically. However, an analytical expression can be developed for the effective dispersion coefficient in turbulent flow when there is no biofilm. Hence, the particle tracking model will be verified for the non-reactive case only. The extension to include a boundary reaction will be presumed to be correct.

The following solution for the effective dispersion coefficient was developed by Taylor in 1954 and was summarized by Fischer in 1979. A solvable form of the advection-dispersion equation for turbulent flow, when written with a coordinate system whose origin moves at the mean flow velocity, is given below (Fischer, 1979):

$$u' \frac{\partial \overline{C}}{\partial \xi} = \frac{1}{r} \frac{\partial}{\partial r} \left(r \varepsilon \frac{\partial C'}{\partial r} \right) \qquad \text{Eq. 3.28}$$

where $\overline{C}$ is the cross-sectionally averaged concentration, *C'* is the deviation from the mean concentration ($C - \overline{C}$), *u'* is the deviation from the mean velocity ($u - \overline{u}$), $\xi = x - \overline{u}t$ (where *x* is the longitudinal direction), and ε is the eddy diffusivity as a function of radial position. Solving Equation 3.28 for *C'* results in the following expression:

$$C' = \frac{\partial \overline{C}}{\partial x} \left[\int_0^r \frac{1}{r \varepsilon} \left(\int_0^r u' r \, dr \right) dr \right] + C'(0) \qquad \text{Eq. 3.29}$$

The rate of mass transport in the streamwise direction, relative to the moving coordinate system, is expressed as:

$$\dot{M} = \int_0^a u' C' 2 \pi r \, dr \qquad \text{Eq. 3.30}$$

Combining Equation 3.29 and Equation 3.30 results in the following:

$$\dot{M} = 2\pi\frac{\partial\overline{C}}{\partial x}\left[\int_0^a u'r\int_0^r\frac{1}{r\varepsilon}\int_0^r u'r\,dr\,dr\,dr\right] \qquad \text{Eq. 3.31}$$

the term $\int_0^a u'rC'(0)dr = 0$ because $\int_0^a u'r\,dr = 0$. The mass transport rate can also be defined in terms of a bulk mass transport coefficient, which would be analogous to the effective dispersion coefficient, by the following equation:

$$\dot{M} = -\pi a^2 D^*\frac{\partial\overline{C}}{\partial x} \qquad \text{Eq. 3.32}$$

Combining Equation 3.31 and Equation 3.32 and solving for D^* gives the following expression for the effective dispersion coefficient:

$$D^* = -\frac{2}{a^2}\int_0^a u'r\int_0^r\frac{1}{r\varepsilon}\int_0^r u'r\,dr\,dr\,dr \qquad \text{Eq. 3.33}$$

Using the velocity and diffusivity profiles described in Section 2.3, and solving Equation 3.33 through numerical integration, gives results that vary with the Reynolds number, $D^* = f(\mathrm{Re})au_*$. Taylor's 1954 analysis results in a value of $10.1au_*$ for the effective dispersion coefficient. This discrepancy is a result of the velocity profiles used in the analysis. Taylor used a velocity profile that did not vary with Reynolds number. Furthermore, the fact that the thickness of the laminar sublayer (wall region) varies with Reynolds number was not accounted for. The velocity profile used in Equation 3.33 is the widely accepted, universal velocity profile which depends on the Reynolds number. Also, the description of the wall region includes variations in thickness dependent on the Reynolds number. Therefore, it is expected that Taylor's result for the effective dispersion coefficient is inconsistent with the solution to Equation 3.33.

Chapter 4

Particle Tracking Results and Verification

For all particle tracking simulations the zeroth, first, and second mass moments are calculated. These are used to compute the asymptotic values for the effective decay, effective velocity, and the effective dispersion coefficients. Three plots are generated to determine the coefficients. The first is a plot of the zeroth moment versus simulation time. In other words, it shows the total mass of the system as a function of time. Since this is a first order decay process, an exponential curve can be fit to the data to determine the rate constant. The first order rate constant is the bulk flow decay coefficient.

The second plot shows the center of mass of the system as a function of time. The center of mass is computed as the first moment of mass divided by the second moment of mass. Once the pseudo steady state conditions have been established (the initial development time has elapsed) the center of mass moves at a constant rate. This is shown as a linear relationship between centroid position and time. The slope of this line is the effective velocity.

The third plot shows the variance of the particle distribution as a function of time. The variance is computed as:

$$\sigma^2 = \frac{M_2}{M_0} - \bar{X}^2(t) \qquad \text{Eq. 4.1}$$

After the initial development period, the variance changes at a constant rate. Once again this is shown by a straight line on the graph. The slope of this line is equal to twice the effective dispersion coefficient (see Equation 1.27).

4.1 Laminar Flow Results

Three simulations were run to give examples of the spatial moment curves and to verify the particle tracking model with analytical results. Simulation 1 used the average values for the biofilm parameters, a first order decay constant of -1.0, a molecular diffusion coefficient of 1.0×10^{-5} cm^2/s, and a mean bulk flow velocity of 6.44 cm/s. Simulation 2 used all the same parameters, except a molecular diffusion coefficient of 5.0×10^{-5} cm2/s. A simulation was also run with no decay occurring in the biofilm (all other parameters are the same as simulations 1). Table 4.1 gives a summary of the simulation results and the corresponding analytical solutions.

Table 4.1: Comparison of Simulations to Analytical Results

	Sim 1	Analytical 1	Sim 2	Analytical 2	No Decay
K_{eff} (1/s)	-9.79×10^{-5}	-9.75×10^{-5}	-4.85×10^{-4}	-4.80×10^{-4}	0.0
U_{eff} (cm/s)	9.93	10.03	9.82	9.90	6.10
D_{eff} (cm^2/s)	12533	12987	2802	2680	59519

The particle tracking results match closely with the analytical solutions. While there are some slight discrepancies, these simulations along with several others (some if which are discussed later) suggest that the particle tracking model accurately describes mass transport in a laminar flow field. There are several reasons why discrepancies may occur. Since the effective transport coefficients are determined by regression analyses of the moment curves, their values are subject to the degree of “fit” of the regression curves. The regression analysis must be performed on the portion of the moment curve that lies after the initial development period. If some of this region

is included in the regression analysis, the accuracy of the result may suffer, albeit very slightly. Basically, the results of the regression analysis depend on the care taken by the person performing them. An increase in the number of particles and a smaller timestep would also lead to more accurate results. However, an effort was made to used as few particles as possible and the largest timestep possible (that will still give accurate results) in order to cut down on simulation run time. Finally, it is entirely possible that the analytical solutions are not exact. Due to the complex nature of the solution, which involves iteration, numerical solutions to find roots of equations, and the summation of results from a theoretically infinite number of eigenvalues, the analytical results themselves are only approximations.

For the same system as simulation 1 with no biofilm the effective decay coefficient is zero, the effective velocity is the mean flow velocity (6.44 cm/s), and the effective diffusion coefficient is 50565 cm^2/s (from Equation 1.6). A reactive biofilm results in a non-uniform concentration distribution across the pipe cross section because particles near the biofilm are subject to decay. Because this is also the region of lowest velocity, the center of mass will travel faster than the mean velocity. Likewise the particles are subject to less separation because most of the mass exists in areas of lower shear. As expected, Table 4.1 shows that the presence of a reactive biofilm causes the effective velocity to increase and the effective dispersion coefficient to decrease. It is interesting to note that the simulation with no decay results in a lower effective velocity than the mean flow and a higher effective dispersion than a pipe with no biofilm. This is because particles may enter the biofilm without losing any mass. In the biofilm the velocity is zero, so particles may lag behind the particles in the bulk flow. This leads to a decreased effective velocity and an increase in particle separation.

It is important to notice that the effective decay coefficient is several orders of magnitude smaller than the biofilm decay coefficient. Since the effective decay represents an overall decay of the mass in the bulk flow, it is expected to be much smaller

than the regional decay rate at the boundary.

The following figures are the spatial, mass moments resulting from simulations 1 and 2. The values reported in Table 4.1 are determined by a regression analysis of these graphs. Figure 4.1 shows the change in mass as a function of time (M = mass and M_t = total mass at the beginning of the simulation) for the two simulations. The effective decay coefficient is determined by fitting and exponential curve to the portion of the curve that resides after the initial development time. The portion of the curve that resides previous to the development time is not a first order function and therefore an exponential curve could not be fit to it.

Figure 4.1: Zeroth Moment Curve

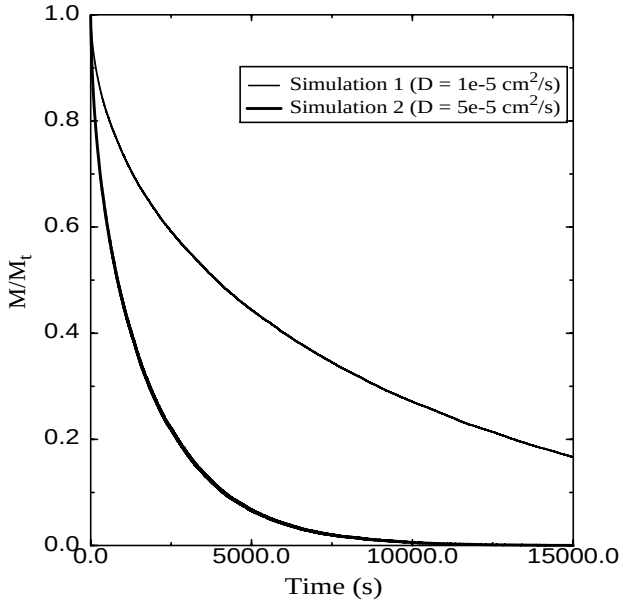

Figure 4.2 and Figure 4.3 can be used to investigate the development times for the respective systems. The development region is a little more obvious in Figure 4.3 than Figure 4.2. It represented by the curved region of the graph before it develops into a straight line. The development time for simulation 1 is approximately 5000 seconds. It is difficult to determine the development time for simulation 2 but it is probably about 1000 seconds. Because the molecular diffusion coefficient is greater for simulation 2, mixing in the radial direction occurs faster. The initial distribution of particles

is therefore “forgotten” in a shorter amount of time and effective one dimensional transport is established more quickly.

It is evident from the two simulations that an increase in the molecular diffusion coefficient leads to a decrease in both the effective dispersion coefficient and the effective velocity. The effective dispersion coefficient decreases because mixing in the radial direction increases. Therefore, particle separation in the longitudinal direction due to the velocity gradient is decreased. For the same reason, the effective velocity decreases. Even though more mass is being transported to the biofilm (which leads to the increase in the effective decay coefficient [see Table 4.1]), the high degree of mixing in the radial direction leads to a more uniform distribution of mass across the cross section. Theoretically, as the molecular diffusion coefficient continues to increase, the effective velocity will approach the mean flow velocity.

Figure 4.2: First Moment Curve

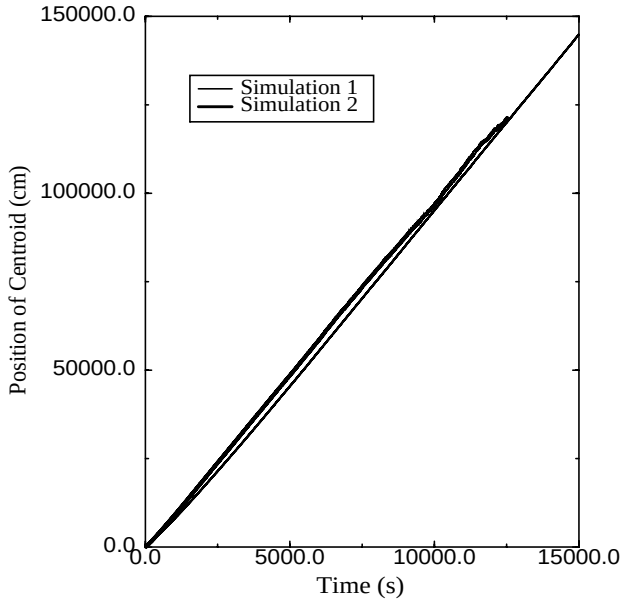

Figure 4.3: Second Moment Curve

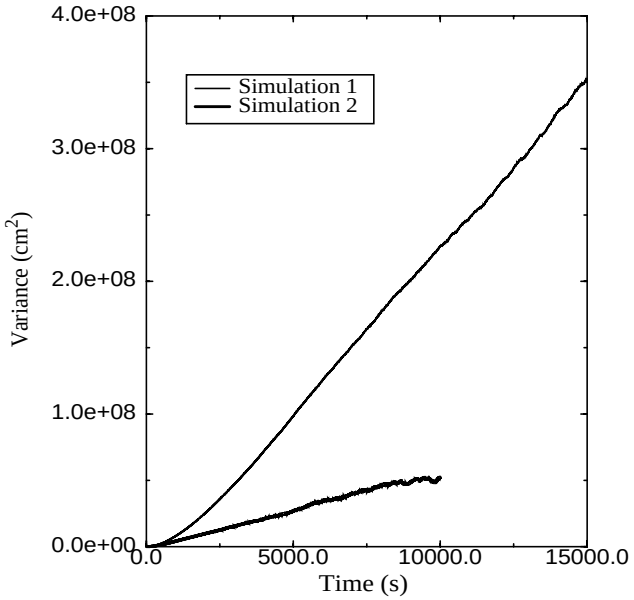

Numerical Issues

There are two model parameters that affect the numerical accuracy of the model results; the timestep length and the number of particles used. The restrictions on timestep length are discussed in detail in Chapter 2. There are no definitive restrictions on the number of particles. However, Tompson suggests that the number of particles necessary for accurate results is on the order of 10^4 (Tompson, 1988). The following two examples demonstrate the numerical inaccuracies that could result if an improper timestep was chosen or too few particles were used. All other parameters are the same as those used in simulation 1, discussed above.

Figure 4.4: Zeroth Moment - Too Few Particles

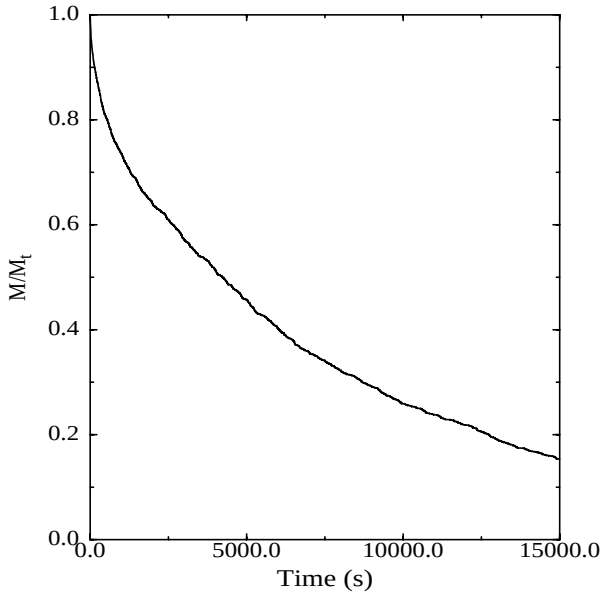

Figure 4.5: Second Moment - Too Few Particles

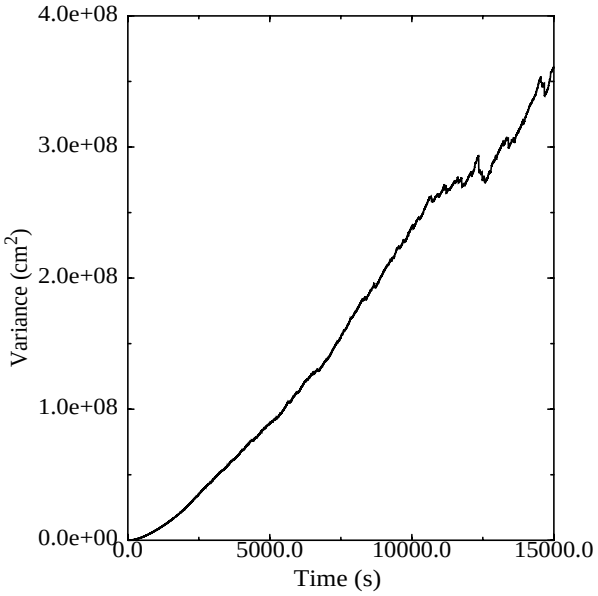

Figure 4.4 and Figure 4.5 show the zeroth and first moments for a simulation using 1500 particles. The number of particles used to obtain the results given for simulation 1 is 24000. It is obvious that the model output does not result in smooth curves for the spatial moments. Performing a regression analysis on the curves to determine the effective bulk transport parameters gives incorrect results (see Table 4.2). Because

the particles are behaving properly (i.e. a proper timestep was used), the discrepancy between the model results and the correct results (those of simulation 1) is not considerable. There are simply not enough particles for the mean motion to represent reality. This explains why the spatial moments do not result in smooth curves. It would be obvious to the model user that the results are not correct.

Table 4.2: Discrepancies from Incorrect Numerical Parameters

	K_{eff} (x 10^{-5}/s)	V_{eff} (cm/s)	D_{eff} (cm^2/s)
Simulation 1	-9.79	9.80	12533
Too Few Particles	-10.7	9.86	13197
Too Large Δt	-9.07	9.59	15831

The simulation used to produce Figure 4.6 and Figure 4.7 used a timestep length of 10 seconds when the appropriate timestep length (that used for simulation 1) is approximately 0.1 seconds (as dictated by the time-space restrictions discussed in Section 2.2). Unlike the results produced by a model with too few particles, a model using an incorrect timestep will result in smooth curves for the spatial moments. As long as there are a sufficient number of particles to get consistent and smooth average particle transport, the moment curves will also be smooth. The behavior of the individual particle however, will be inconsistent with reality. For example, a particle could move from the center of the pipe to the pipe wall in a single diffusion step. Therefore, even though the spatial moment curves may look correct, a regression analysis of these curves would give highly inaccurate values for the effective bulk transport coefficients. The results in Table 4.2 show that this is indeed the case. A model user would have no way of knowing that the results are inaccurate unless they were compared with an analytical model. Therefore, it is imperative that the timestep restrictions discussed in

Table 2.2 are strictly adhered to. Another way to determine a proper timestep is to perform several simulations, decreasing the timestep length in each one. When a decrease in timestep fails to change the results, a valid timestep length has been determined (Once an appropriate timestep has been determined, a decrease in timestep length of any amount will not change the model results significantly. There will always be slight variations due to the random nature of particle tracking models). This is a very time consuming and impractical way to choose the timestep length however.

Figure 4.6: Zeroth Moment - Large Δt

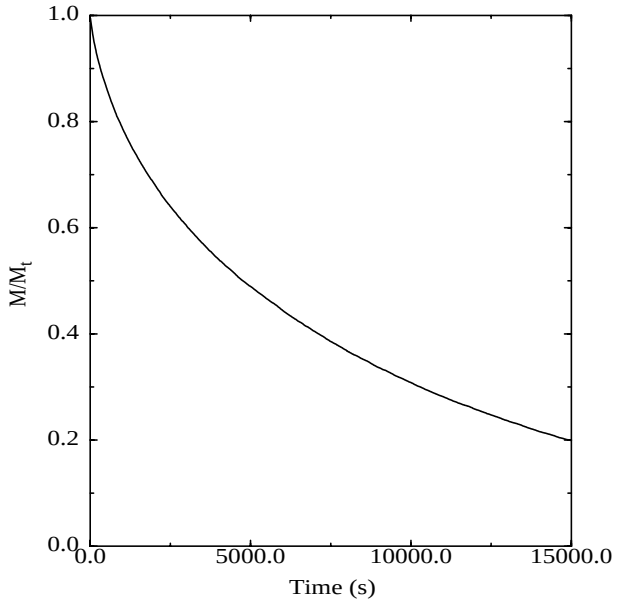

Figure 4.7: Second Moment - Large Δt

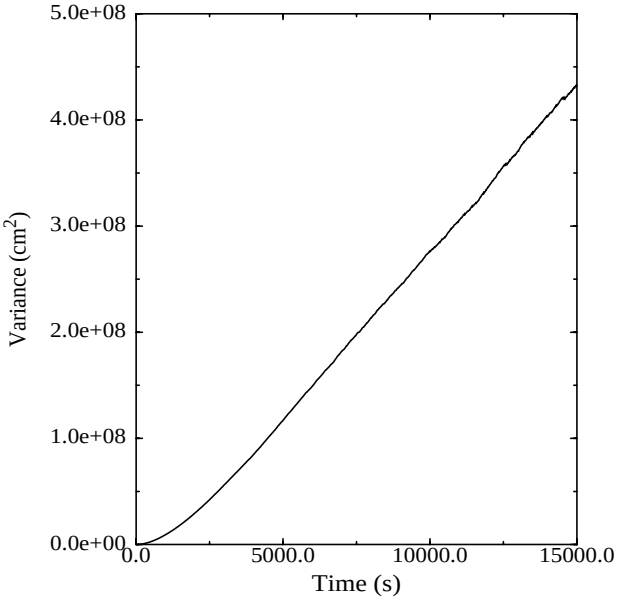

Dependence of Transport Parameters on Reynolds Number

In order to simulate the Horn and Hempel experiments, a system was constructed using the average values for porosity, D_{bio}/D, biofilm thickness and molecular diffusion given in Chapter 2. A first order decay constant of -1.0/s was used and a pipe radius of 0.8 cm. Simulations were then performed for Reynolds numbers in the range of 536 - 2000.

Table 4.3: Mass Transport Parameters for a Range of Reynolds Numbers

Reynolds Number	Mean Velocity (cm/s)	K_{eff} (x 10^{-5}/s)	U_{eff} (cm/s)	D_{eff} (cm^2/s)
536	3.3	-9.70	5.11	3358
650	4.0	-9.60	6.2	4976
800	4.93	-9.60	7.7	7544
900	5.8	-9.64	9.04	10475
1300	8.37	-9.60	13.1	21790
1700	10.9	-9.64	17.1	37365
2000	12.9	-9.58	20.1	51389

Contrary to the results of the Horn and Hempel experiments, the effective decay constant does not vary with Reynolds number. As discussed in Chapter 1, the effective decay constants measured and computed for the Horn and Hempel experiments are not the asymptotic values. Therefore, they are expected to vary with Reynolds number because they are dependant on the entrance development and the reactor travel time. Since the values computed by the particle tracking model are the asymptotic transport parameters, the effective decay will not vary with Reynolds number.

Both the effective velocity and the effective dispersion coefficient increase with increasing Reynolds number. Since the mean velocity of flow in the pipe increase with Reynolds number (by definition), the effective velocity is also expected to increase. The effective velocity is always greater than the mean velocity because the particles near the wall of the pipe (where the velocity is lowest) are subject to decay. Therefore, the most mass will exist in the center of the pipe where the velocity is higher than the mean velocity. The effective dispersion coefficient increases with increasing Reynolds numbers because the velocity profile is more spread out in the axial direction for high Reynolds numbers. In other words, the centerline velocity increases with increasing Reynolds number but the velocity at the wall is always zero. Therefore two particles, one at the center of the pipe and one at the wall, will spread apart faster when the centerline velocity is high, than the same two particles when the centerline velocity is low.

Sensitivity to Porosity and D_{bio}/D

Since it is difficult to precisely define the physical structure of a biofilm, parameters such as the porosity and biofilm diffusion coefficient (which are usually the most difficult to determine) have to be estimated with some degree of uncertainty. The average value from literature may be used or the parameter could be set as a result of calibration. Either way, it is useful to know how sensitive a model is to the most

uncertain parameters. If it turns out that a model is very sensitive to these parameters, then there would be justification in performing various experiments to measure them in a more accurate manner. However, if it turns out that the model is not really affected by these parameters, then it is probably safe to use an average value. Table 4.4 and Table 4.5 show the sensitivity of the bulk transport parameters to porosity. All other parameters are held constant at the average value discussed at the end of Chapter 2. The radius of the pipe is 0.8 cm, the Reynolds number is 1000 and the first order decay constant in the biofilm is -1.0.

Table 4.4: Porosity Sensitivity Analysis - Particle Tracking Model

Porosity	K_{eff} (x 10^{-5}/s)	U_{eff} (cm/s)	D_{eff} (cm^2/s)
.4	-9.42	9.92	14220
.5	-9.85	9.92	13800
.65	-9.65	9.97	13300
.8	-9.77	10.05	12584
.95	-9.67	9.96	13115
1.0	-9.56	10.05	12307

Table 4.5: Porosity Sensitivity Analysis - Analytical Model

Porosity	K_{eff} (x 10^{-5}/s)	U_{eff} (cm/s)	D_{eff} (cm^2/s)
.4	-9.62	9.99	13042
.5	-9.67	10.01	12593
.65	-9.72	10.02	13106
.8	-9.75	10.03	12850
.95	-9.77	10.04	12677
1.0	-9.78	10.04	12656

Table 4.4 and Table 4.5 show that porosity does not have a significant impact

on the bulk transport parameters. A change in porosity of ±43% (from the mean) results in the following percent changes in the bulk transport parameters: ±0.8% in K_{eff} for the analytical model, ±2.2% in K_{eff} for the particle tracking model, ±0.25% in U_{eff} for the analytical model, ±0.65% change in U_{eff} for the particle tracking model, ±1.5% in D_{eff} for the analytical model, and ±7.5% in D_{eff} for the particle tracking model.

While the bulk flow transport parameters appear to be relatively insensitive to changes in porosity, there are some noticeable trends. An increase in porosity results in an increase in K_{eff} and U_{eff}, but a decrease in D_{eff}. At higher porosities, particles are able to enter the biofilm more readily. This is also reflected in the probability rule expressed by Equation 2.15, and is consistent with the behavior expected due to increased porosity of the biofilm. If more particles are allowed to enter the biofilm, the effective decay coefficient would naturally increase. This results in less solute mass near the biofilm (where the velocity is lowest and the shear is the greatest). Therefore, the effective velocity increases and the effective dispersion decreases.

It is important to note that the particle tracking model is not accurate enough to correctly predict the sensitivity to porosity. While it is still evident that the system is relatively insensitive to changes in porosity, the trends shown in the analytical results are not as obvious in the particle tracking results. In fact one could say that the particle tracking model is unable to accurately portray these trends. The reason for this inaccuracy is the random nature of the model. Even with the same input parameters, the particle tracking model could return slightly different results (each simulation different random numbers are generated). In this case, the differences caused by the random nature of the model overshadow the differences caused by porosity variations. This problem would be resolved by increasing the number of particles used in the simulation.

Table 4.6 and Table 4.7 show the sensitivity of the bulk transport parameters to the ratio of the biofilm diffusion coefficient to bulk flow diffusion coefficient (D_{bio}/D).

All other parameters are kept constant and are the same as those used in the porosity sensitivity analysis.

Table 4.6: Sensitivity to D_{bio}/D - Particle Tracking Model

D_{bio}/D	K_{eff} (x 10^{-5}/s)	U_{eff} (cm/s)	D_{eff} (cm^2/s)
.35	-9.94	9.97	12462
.5	-9.85	9.97	13105
.65	-9.69	9.97	13000
.8	-9.46	10.04	12812
.9	-9.69	9.99	13144

Table 4.7: Sensitivity to D_{bio}/D - Analytical Model

D_{bio}/D	K_{eff} (x 10^{-5}/s)	U_{eff} (cm/s)	D_{eff} (cm^2/s)
.35	------	-------	-------
.5	-9.73	9.8	13100
.65	-9.75	10.06	12954
.8	-9.76	10.05	12834
.9	-9.77	10.03	12757

The results of the sensitivity analysis to D_{bio}/D are similar to the porosity sensitivity analysis. The system is not very sensitive to changes in the ratio D_{bio}/D, even less so than porosity. The role of the biofilm diffusion coefficient is twofold. First, and most obvious is dictates the extent of diffusion occurring in the biofilm. Second, like porosity, it affects the interface condition. If the ratio D_{bio}/D is close to one, a particle may diffuse readily into either the bulk flow or the biofilm from the interface. The lower this ratio gets however, the less likely the chance that a particle will diffuse to the biofilm. For this reason, the same trends are apparent here as in the porosity sensi-

tivity analysis. Once again, the particle tracking model is not sensitive enough to display these trends.

An important point to consider in this analysis is that the sensitivity results apply to the specified system only. If the set of system parameters were to change, the sensitivity analysis would also likely change. For example, the system just described is mostly diffusion limited. This means that the bulk flow transport parameters are largely affected by the rate at which solute can reach the biofilm. If the sensitivity analysis was performed on a rate limited system (the bulk flow transport parameters are largely affected by the reaction rate in the biofilm), the results would show a greater sensitivity to both porosity and D_{bio}/D. Likewise, a system with a thicker biofilm would probably show greater sensitivity to D_{bio}/D than a system with a thin biofilm. This hypothesis will be tested further in the next section.

Diffusion Limited Versus Rate Limited Systems

A diffusion limited system is one in which the ratio of the biofilm decay rate to diffusive flux is high. In other words, the effective decay is governed by how fast mass can be transported from the bulk flow into the biofilm where it would decay almost instantly. When a system is limited by diffusion, an increase in the biofilm decay rate does not have a significant effect on the bulk transport parameters. Conversely, in a rate limited system, depleted mass is quickly replenished by diffusion from the bulk flow. The ratio of the biofilm decay rate to diffusive flux is low. Therefore the bulk flow effective decay is dictated by the decay rate in the biofilm.

It is believed that the system used to perform the previous sensitivity analysis on porosity (shown in Table 4.4 and Table 4.5) was limited by diffusion. For comparison, the same analysis was performed for a rate limited system. The results are shown in Table 4.8 and Table 4.9.

Table 4.8: Porosity Sensitivity - Rate Limited Particle Tracking Model

Porosity	K_{eff} (x 10^{-4}/s)	U_{eff} (cm/s)	D_{eff} (cm^2/s)
.4	-2.54	9.67	6439
.5	-2.62	9.72	5432
.65	-2.7	9.78	5364
.8	-2.75	9.84	4948
.95	-2.76	9.87	4722

Table 4.9: Porosity Sensitivity - Rate Limited Analytical Solution

Porosity	K_{eff} (x 10^{-4}/s	U_{eff} (cm/s)	D_{eff} (cm^2/s)
.4	-2.56	9.64	6134
.5	-2.64	9.73	5694
.65	-2.71	9.81	5277
.8	-2.76	9.86	5023
.95	-2.79	9.89	4857

It is obvious that the particle tracking model is much more accurate for this set of simulations. The results match the analytical solutions very closely (except for the effective dispersion which is believed to be slightly inaccurate in the analytical model). It is believed that the reason for the lack of accuracy in the diffusion limited analysis has to do with the number of particles used. In a rate limited system the diffusive flux in the radial direction is high. Therefore, there is a very large number of particle collisions with the bulk flow - biofilm interface. Because the number of collisions is so high, the simulated particle behavior at the interface, as dictated by the probability rule, will more accurately depict the expected average behavior at the interface. For

the diffusion limited system, the same number of particles was used in the simulation, however, there were far fewer collisions with the interface. Therefore, there were not enough collisions to result in the proper average behavior.

It is also apparent that the rate limited system is more sensitive to porosity. Table 4.10 gives a summary of the sensitivity analyses for the two systems.

Table 4.10: Summary of Sensitivity Analysis

	Change in Porosity	Change in K_{eff}	Change in U_{eff}	Change in D_{eff}
Diffusion Limited	±40.7%	±0.82%	±0.25%	±1.5%
Rate Limited	±40.7%	±4.2%	±1.0%	±15.4

As expected, the model is more sensitive to porosity for a rate limited system than a diffusion limited system. As previously discussed, for a diffusion limited system the effective bulk flow parameters are largely dictated by the diffusive flux to the biofilm. Therefore, it is expected that the system will not be very sensitive to biofilm parameters. However, in a rate limited system, there is always ample mass at the biofilm interface. What happens to that mass is largely a result of the biofilm parameters. Hence, the system is more sensitive to changes in porosity.

Effects of Diffusion Limitation

The Damkohler number is a dimensionless number defined as ka^2/D. It is used in the following figures to show the relationships between the effective transport parameters and the ratio of decay to diffusion. Figure 4.8 shows the relationship between K^*/K_{max} and the Damkohler number for different values of a/b. K_{max} represents the overall decay in the absence of diffusion limitations. It is calculated as the cross sectionally averaged decay rate (biofilm decay rate multiplied by the ratio of biofilm cross sectional area to total cross sectional area).

Figure 4.8: Effective Decay vs. Da

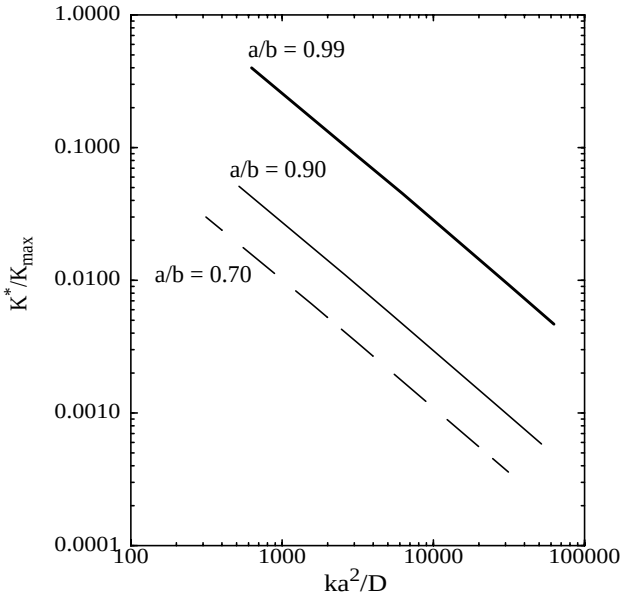

The effects of diffusion limitations on the effective decay are apparent. As the system becomes more diffusion limited (the Damkohler number increases), the effective decay becomes further from the maximum decay. Conversely, as diffusion limitations decrease, the effective decay approaches the maximum decay.

Figure 4.9 shows the effects of diffusion and decay on the effective velocity. As the decay rate approaches zero or as the diffusion coefficient becomes very large the effective velocity approaches the mean velocity as expected. Also, it is apparent that an increase in decay rate, beyond a certain point, causes no further increase in effective decay.

Figure 4.9: Effective Velocity vs. Da

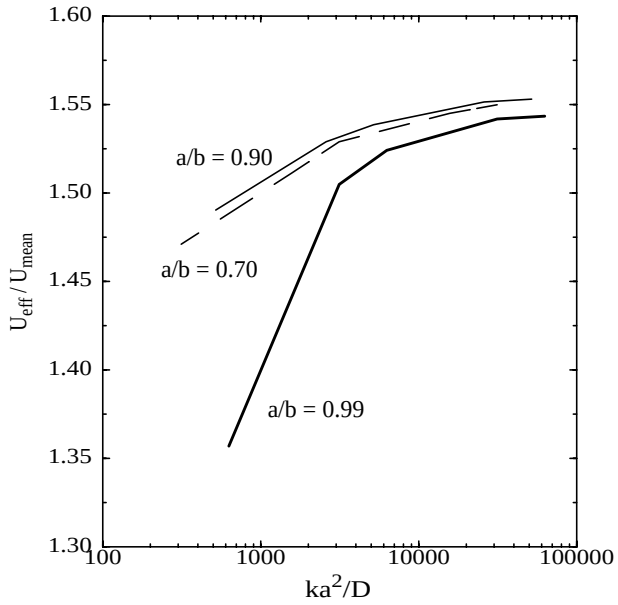

Figure 4.10 shows the relationship between D^*/D_{Taylor} and the Damkohler number. D_{Taylor} is the effective dispersion coefficient for a pipe without a biofilm (calculated by Equation 1.6). As the effects of the biofilm become more and more insignificant, the effective dispersion coefficient approaches the Taylor dispersion coefficient (This behavior is also apparent in Table 4.1). As with the effective velocity, there seems to be a decay value beyond which the an increase in decay produces no further decrease in effective dispersion.

Figure 4.10: Effective Dispersion vs. Da

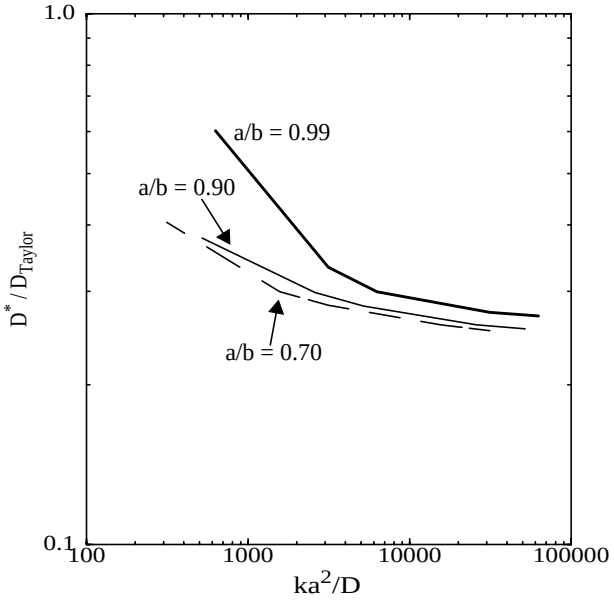

4.2 Turbulent Flow Results for a Smooth Pipe

The turbulent flow models generate the same output as the laminar flow models. Zeroth, first, and second mass moment curves are used to determine the effective transport parameters through regression analysis. Since there is considerable interest in turbulent pipe flow systems with no reactive biofilm, simulations were performed to characterize transport in turbulent flow with and without a boundary reaction.

Turbulent Transport With No Boundary Reaction

A set of simulations were used to compare the particle tracking results with Taylor's 1954 turbulent flow results. The analytical solution, discussed in Chapter 3, is used to verify the particle tracking model. The following simulations, shown in Table 4.11, were performed with a pipe radius of 4.0 cm and a molecular diffusion coefficient of 1.0×10^{-5} cm^2/s. The Reynolds number was varied to show its effect on the effective longitudinal dispersion coefficient.

Table 4.11: Effect of Reynolds Number on Effective Dispersion

Reynolds Number	Effective Dispersion (Particle Tracking)	Effective Dispersion (Analytical Solution)
10000	$29.3au_*$	$29.3au_*$
50000	$8.1au_*$	$8.0au_*$
100000	$6.5au_*$	$6.1au_*$
500000	$5.7au_*$	$5.3au*$
1000000	$5.3au_*$	$5.1au*$

The effect of Reynolds number on the asymptotic longitudinal dispersion coefficient is apparent. At lower Reynolds numbers, the laminar sublayer is considerably thicker. Therefore, more solute mass can become trapped in the sublayer and separated from the mass in the turbulent core. As the Reynolds number increases, however, the laminar sublayer becomes extremely thin and is unable to hold a considerable amount of mass. Therefore the laminar sublayer, and changes in the Reynolds number itself, will have very little impact on the effective dispersion coefficient at high Reynolds numbers.

It is obvious that Taylor's result, $D^* = 10.1au_*$, does not apply for the velocity and diffusivity distributions used in this research. The velocity profile, and hence the diffusivity profile, used by Taylor does not vary with Reynolds number. Therefore, his analysis results in a constant, 10.1, multiplied by au_*. The velocity profile used in the particle tracking and analytical models does vary with Reynolds number, hence the discrepancy with Taylor's result is expected. In the field of Civil Engineering, no studies have been performed to verify Taylor's result (since Taylor's experimentation in 1954). However, there has been considerable research attempting to develop expressions for velocity and diffusivity in the wall region. The velocity and diffusivity profiles used in this research (Wasan and Wilke, 1964), are accepted as a more accurate description of transport in the wall region than Taylor's. It is then reasonable to assume

that the results given by the particle tracking model provide a better representation of dispersion in turbulent pipe flow than Taylor's result. However, experimental results are required to confirm this hypothesis.

Taylor's experimental results vary from $10.6au_*$ to $12.8au_*$. These experiments were run for Reynolds numbers near 20000 without much variation. The particle tracking model gives a value of approximately $14au_*$ for a Reynolds number of 20000. The model results therefore seem to overprotect the dispersion seen in Taylor's experiments. It is possible that the velocity profile used in Taylor's analysis was developed from the profile seen in the experiments. This would explain the close correlation between the theory and experimentation. Since the Reynolds number was not varied greatly, the relationship between Reynolds number and effective dispersion went unnoticed. However, before any final conclusions can be reached on this issue, additional physical experimentation should be performed for a wide range of Reynolds numbers.

Turbulent Transport with a Reactive Biofilm

Once the turbulent flow model was verified analytically for the non-reactive case, it was extended to include a boundary reaction. No analytical solutions are available for this system so there is currently no way to verify these results. Physical experimentation is necessary in order to ensure that the model is working properly.

Four simulations were run to show the effects of a reactive biofilm and to compare the results to a similar system with no biofilm and a system with a non-reactive biofilm. The simulations were run with at a Reynolds number of 100,000, a pipe radius b of 5.0 cm, a biofilm thickness of 0.3 cm (a = 4.7), a first order decay constant of -15.0 s^{-1}, porosity of 0.73, and D/D_b of 0.6. This results in a mean flow velocity of 104.3 cm/s and a shear velocity of 4.94 cm/s. The required timestep for this system is 0.0001 seconds and 50,000 particles were used in the simulation. The total observation

time for the simulation is 40 seconds. Since the degree of transverse mixing in a turbulent system is several orders of magnitude larger that a laminar system, the initialization time is much smaller. The asymptotic value of the effective transport parameters is reached within a few seconds. Since the simulation time is so short, the first order decay constant must be much larger that the usual value in order to get an appreciable amount of decay. Table 4.12 shows the results of the four simulations. Simulation 1 uses a molecular diffusion coefficient of $1x10^{-5}$ cm^2/s and simulation 2 uses a diffusion coefficient of $1x10^{-4}$ cm^2/s.

Table 4.12: Turbulent Flow Results with Biofilm

	Simulation 1	**Simulation 2**	**No Biofilm**	**No Decay**
K_{eff} (1/s)	-1.05×10^{-3}	-4.16×10^{-3}	0.0	0.0
U_{eff} (cm/s)	104.33	104.55	104.13	103.74
D_{eff} (cm^2/s)	$5.78au_*$	$5.48au_*$	$6.6au_*$	$49.0au_*$

It is apparent that a reactive biofilm has the same effects on a turbulent flow system as a laminar flow system, however much less pronounced. The boundary reaction results in a non-uniform cross-sectional solute concentration. Therefore, the effective velocity is expected to increase and the effective diffusion is expected to decrease. This trend is clearly seen in Table 4.12. While the reactive biofilm does cause the expected changes in effective velocity and effective dispersion, the changes are very slight. This is because the rate of radial dispersion in a turbulent flow system is very large. Even though the biofilm is reducing the solute mass at the boundary, it is quickly replenished by dispersion from the turbulent core. Therefore, a the cross-sectional solute concentration remains nearly uniform. The simulation with a non-reactive biofilm also gives the expected results. Mass that enters the biofilm in this case has zero advection but does not decay. Therefore particles in the biofilm quickly becomes separated from those in the bulk flow. This causes a decrease in effective velocity and an increase

in effective dispersion.

The differences between Simulation 1 and Simulation 2 are due to the difference in the molecular diffusion coefficient. A change in molecular diffusion of one order of magnitude only produces slight changes in the effective transport parameters. It is then obvious that the role of the molecular diffusion coefficient in a turbulent flow system is much different from its role in a laminar flow system. In a laminar flow field, transport in the radial direction occurs as a result of molecular diffusion only. However, in a turbulent system, radial transport is governed by the turbulent eddies existing within the flow field. Recall from Chapter 2 that the radial dispersion is a function of the slope of the velocity profile, which is several orders of magnitude larger than the molecular diffusion coefficient. Only in the laminar sublayer, very close to the biofilm, does the molecular diffusion coefficient have an impact. Even so, the effects of molecular diffusion are obvious. The laminar sublayer controls the transport of solute into the biofilm. As the molecular diffusion increases, more solute will enter the biofilm. Therefore, the effective decay rate should increase. As decay increases the amount of mass located in the region of lowest velocity and highest shear (near the boundary) decreases. This causes an increase in the effective velocity and a decrease in effective dispersion. These trends are clearly seen in Table 4.12.

Reynolds Number Dependence

Table 4.13 shows the effects of Reynolds number on the effective transport parameters. The apparent trends are the result of changes in the laminar sublayer thickness. As the Reynolds number increases the laminar sublayer thickness decreases. Therefore, the rate of diffusion into the biofilm increases. This results in an increase in the effective decay coefficient. As the laminar sublayer thickness decreases, radial transport in the wall region of the pipe increases. Therefore, a more uniform concentration distribution is maintained throughout the pipe cross section and the effective

velocity approaches the mean flow velocity. For the same reason the effective dispersion coefficient approaches the value seen in the absence of a biofilm.

Table 4.13: Dependence of Transport Parameters on Reynolds Number

Reynolds Number	K_{eff} (1/s)	U_{eff} / U_{avg}	D_{eff} / D_{NB}
10,000	-1.88×10^{-4}	1.008	0.47
50,000	-6.32×10^{-4}	1.0007	0.80
100,000	-1.05×10^{-3}	1.0001	0.89
500,000	-3.10×10^{-3}	1.0	0.96
1,000,000	-3.30×10^{-3}	1.0	0.99

Figure 4.11 and Figure 4.12 graphically depict the results given in Table 4.13. In both figures it is apparent that the Reynolds number ceases to have a significant impact after a certain value. This is because the laminar sublayer becomes extremely thin to the point where it is virtually un-noticeable. For the effective decay coefficient, this means that solute can easily enter the biofilm and a rate limited situation is established. For the effective decay coefficient, a high degree of radial mixing exists throughout the entire cross section of the pipe and a concentration distribution that is very near uniform can be maintained.

Figure 4.11: Effect of Reynolds Number on Effective Decay

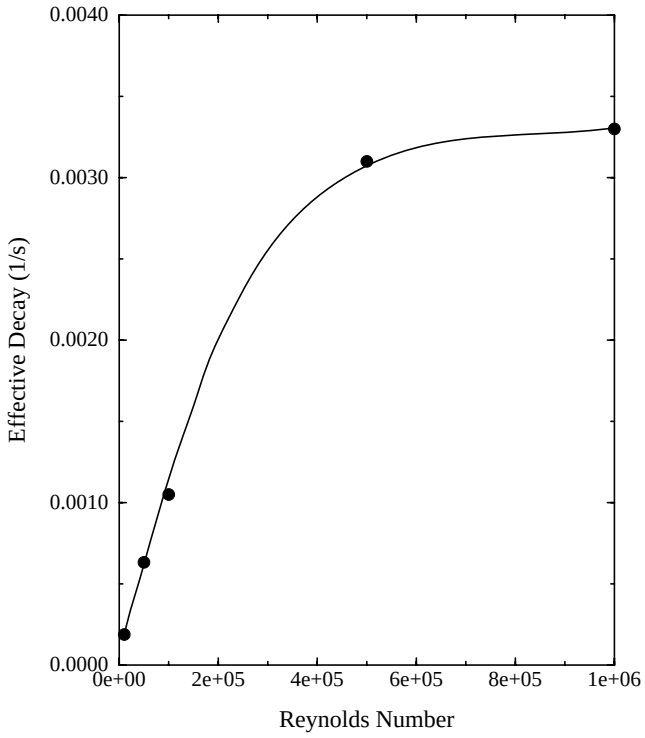

Figure 4.12: Effect of Reynolds Number on Effective Dispersion

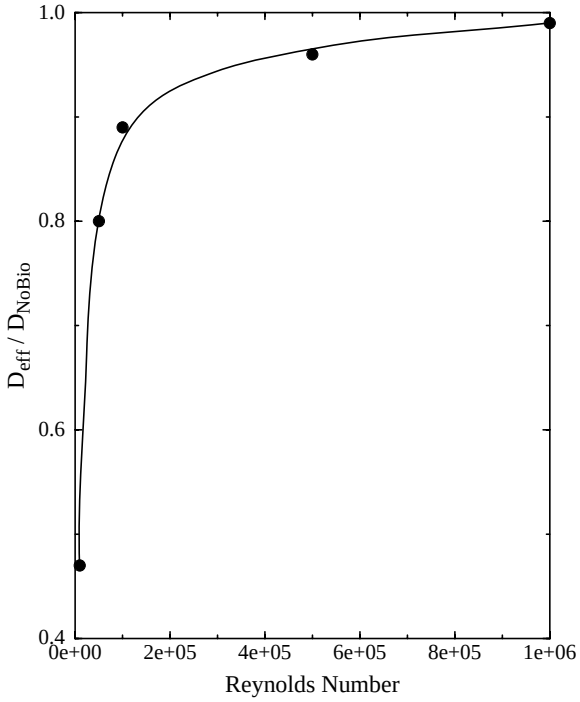

Sensitivity to Damkohler Number

As with the laminar flow model, the effects of diffusion limitations on the turbulent flow effective parameters are examined through the dimensionless Damkohler number. For turbulent flow, the Damkohler number is computed as ka^2/D where D is the average value of the radial dispersion coefficient.

Figure 4.13 shows the relationship between the Damkohler number and effective decay for two ratios a/b and for two different Reynolds numbers. At low Damkohler numbers the system is rate limited and the effective decay approaches the maximum decay seen in the absence of diffusion limitations. At high Damkohler numbers the system is more diffusion limited and the effective decay is much smaller than the maximum decay. These results are almost identical to those seen in the laminar flow case (Figure 4.8).

Figure 4.13: Effective Decay vs. Damkohler Number

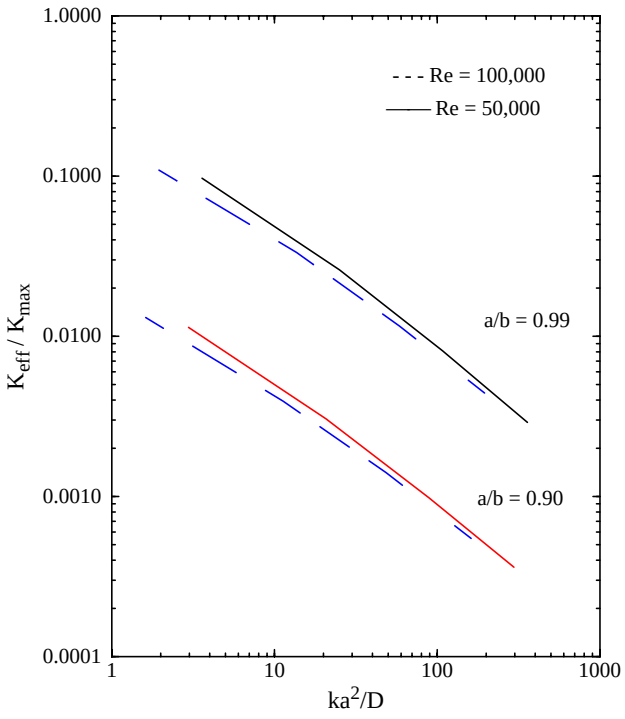

The influence of the Damkohler number on effective velocity is not shown because the variations in effective velocity are too small to display in a graphically

meaningful way. In turbulent flow, the effective velocity is always very close to the mean flow velocity (differences on the order of 10^{-2} - 10^{-3}).

Figure 4.14 shows the relationship between the Damkohler number and the effective dispersion coefficient. The figure shows the results for two different Reynolds numbers for an *a*/*b* ratio of 0.9. Only one *a*/*b* ratio is displayed because the results for different ratios are almost identical. The general trend shown in the figure is similar to that seen in the laminar flow case (Figure 4.10). In a rate limited scenario (low Damkohler number), the concentration distribution is nearly uniform, so the effective dispersion approaches and actually exceeds the dispersion value for the no biofilm case. The reason that the effective dispersion value exceeds D_{NoBio} is due to a storage effect in the biofilm. At low Damkohler numbers, mass is entering the biofilm but it is not decaying very fast. Therefore, mass is stored in the biofilm and is quickly separated from mass in the bulk flow. In a diffusion limited scenario, less mass exists near the pipe wall where the shear is greatest. Therefore, there is less longitudinal separation of particles and the effective dispersion coefficient decreases from the dispersion seen in the absence of a biofilm.

Figure 4.14: Effective Dispersion vs. Damkohler Number

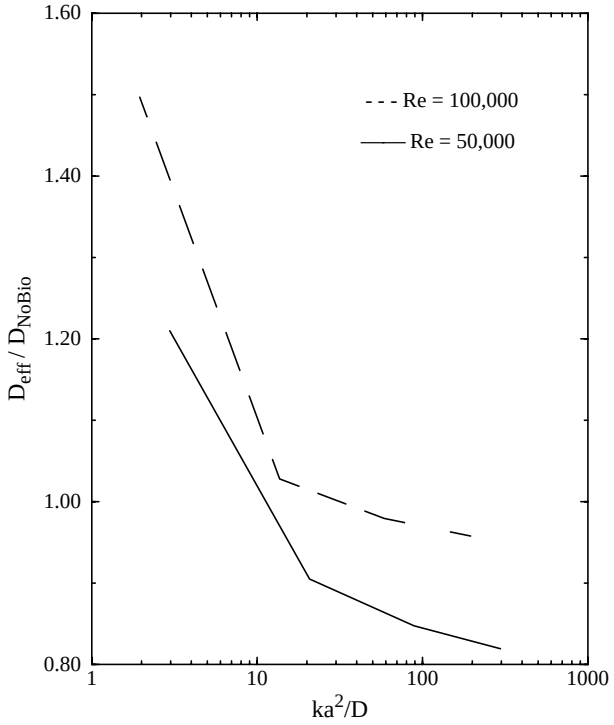

Chapter 5

Conclusion

A particle tracking model was used to quantify the effective transport parameters in a circular pipe with a reactive biofilm. First order kinetics were used to model decay in the biofilm region. Solute transport under laminar flow conditions was examined and verified with the analytical solutions developed by Cox (1997). A turbulent flow model was used to examine solute transport with and without the effects of a reactive biofilm. For the case of turbulent flow without a biofilm, the effective dispersion coefficient was compared with Taylor's result of $10.1au_*$. Using more recently accepted velocity profiles in the turbulent core and the wall region, it becomes apparent that Taylor's result is not valid for a range of Reynolds numbers.

Under laminar flow conditions, the model results provide considerable insight into the relationship between biofilm characteristics and the effective bulk flow parameters. It is shown that a reactive biofilm results in a non-uniform distribution of solute across the pipe cross section. Since less solute mass exists near the pipe wall, the effective velocity is greater than the mean velocity and the effective dispersion is less than the dispersion in a pipe with no biofilm. A sensitivity analysis to porosity and D/D_b shows that the model is not very sensitive to changes in these two parameters. However, the sensitivity is greater in rate limited systems than in diffusion limited systems. In general, as the reactive potential in the biofilm increase, whether through an

increased decay rate, increased porosity, or biofilm thickness, the effective decay and velocity tend to increase and the effective dispersion tends to decrease.

For comparison with the Horn and Hempel experiments, simulations were performed for a wide range of Reynolds numbers. Contrary to the Horn and Hempel results, the effective decay coefficient does not depend on the Reynolds number. It is apparent that the Horn and Hempel experiments are observing pre-development effective decay coefficients. Therefore, their expression for the mass transfer coefficient does not represent the asymptotic effective decay rate that may be used in an effective one-dimensional advection-diffusion reaction equation.

The development of the turbulent flow models required research into the nature of the velocity profile and eddy diffusivity in the wall region of the pipe. The well-known universal velocity profile was used in the turbulent core. In the laminar sublayer, expressions developed by Wasan, Wilke, and Tien (1963) were used to describe the velocity and eddy diffusivity. Using these profiles, a particle tracking model was constructed to determine the effective dispersion coefficient for a pipe with no biofilm. The results were verified by an analytical solution based on Taylor's analysis and were compared to his expression of $10.1au_*$ for the effective dispersion coefficient. Since the velocity profiles used in the particle tracking model varied with Reynolds number, the resulting effective dispersion coefficient should also with Reynolds number. This relationship was clearly seen in the model results and the "constant" 10.1 was actually much higher for low Reynolds number and was lower for high Reynolds numbers. Taylor's analysis, however, was based on a velocity profile which did not change with Reynolds number. Hence, his analysis was unable to capture the effects of changes in the laminar sublayer thickness at different Reynolds numbers. Since the physical experiments used to verify Taylor's analysis did not include a wide range of Reynolds numbers, this behavior went unnoticed. It is probable that the velocity profile used in Taylor's result was developed from velocity data seen in the pipe experiments (or from

an experiment performed at similar Reynolds numbers). Therefore, this topic should be re-examined with additional physical experimentation for a wide range of Reynolds numbers.

Simulations were also performed to analyze the influence of a reactive biofilm on the effective transport parameters in a turbulent flow field. Since no previous research has been done in this area, and no analytical solutions to this problem exist, the particle tracking results could not be verified. Similar trends between the biofilm parameters and the bulk transport parameters were seen in the turbulent flow model and the laminar flow model. The presence of a reactive biofilm results in a non-uniform, cross sectional concentration distribution. Therefore, the effective velocity increases from the mean velocity and the effective dispersion decreases from the dispersion in a pipe with no biofilm. The variations in the effective parameters, however, are much less pronounced in the turbulent flow model than in the laminar flow model. Since there is considerable lateral mixing due to turbulent eddies, a cross sectional concentration distribution that is very near uniform is always maintained. Therefore, the biofilm only affects a very small region of flow near the pipe wall (namely the laminar sublayer). As the Reynolds number increases, the thickness of this region decreases and the effects of the biofilm become less significant. For this reason, and unlike the laminar flow system, the effective decay rate in a turbulent flow system varies with Reynolds number.

References

(Aris, 1956)

Aris, R. 1956. *On the Dispersion of a Solute in a Fluid Flowing Through a Tube*. Proc. R. Soc. London Ser. A 235.

(Chapra, 1997)

Chapra, Steven C. 1997. Surface Water-Quality Modeling. The McGraw-Hill Companies Inc., United States of America.

(Cox, 1997)

Cox, T.J. 1997. *Investigation and Quantification of Boundary Reaction Effect on Solute Transport Parameterization*. University of Colorado at Boulder. Boulder, Colorado.

(Fischer, 1979)

Fischer, H.B., et.al. 1979. Mixing in Inland and Coastal Waters. Academic Press Inc., Boston, MA.

(Horn and Hempel, 1995)

Horn, H., Hempel, D.C. 1995. *Mass Transfer Coefficients for an Autotrophic and a heterotrophic Biofilm System*. Water Science Technology. Vol. 32. No. 8. pp 199-204.

(Li and Chen, 1994)

Li, S., Chen, G.H. 1994. *Modeling the Organic Removal and Oxygen Consumption by Biofilms in an Open-Channel Flow.* Water Science Technology. Vol. 30. No. 2. pp 53-61.

(Taylor, 1953)

Taylor, G.I. 1953. *Dispersion of Soluable Matter in Solvent Flowing Slowly Through a Tube*. Proc. R. Soc. London Ser. A 219.

(Taylor, 1954)

Taylor, G.I. 1954. *The Dispersion of Matter in Turbulent Flow Through a Pipe*. Proc. R. Soc. London Ser. A 223.

(Tompson, 1988)

Tompson, Andrew, et.al. 1988. *Numerical Simulation of Solute Transport in Randomly Heterogeneous Porous Media: Motivation, Model Develpment, and Application*. Department of Civil Engineering. Massachusetts Institute of Technology. Cambridge, Massachusetts.

(Wasan and Tien, 1963)

Wasan, D.T., Tien, C.L., and Wilke, C.R. 1963. *Theoretical Correlation of Velocity and Eddy Viscosity for Flow Close to a Pipe Wall*. A.I.Ch.E. Journal.

(Wasan and Wilke, 1964)

Wasan, D.T. and Wilke, C.R. 1964. *Turbulent Exchange of Momentum, Mass, and Heat Between Fluid Streams and Pipe Wall*. Int. J. Heat Mass Transfer, Vol. 7, pp. 87-94.

(Wilkes, 1999)

Wilkes, J.O. 1999. Fluid Mechanics for Chemical Engineers. Prentice-Hall, Inc., Upper Saddle River, New Jersey.

(Zhang and Bishop 1, 1994)

Zhang, Tian C., and Bishop, Paul L. 1994. *Density, Porosity, and Pore Structure of Biofilms*. Water Research. Vol. 28. No. 11. pp 2267-2278.

(Zhang and Bishop 2, 1994)

Zhang, Tian C., and Bishop, Paul L. 1994. *Evaluation of Tortuosity Factors and Effective Diffusivities in Biofilms*. Water Research. Vol. 28. No. 11. pp 2279-2287.